JOURNAL OF GEOPHYSICAL RESEARCH, VOL. 112, G02015, doi:10.1029/2006JG000227, 2007

Role of nitrification and denitrification on the nitrous oxide cycle in the eastern tropical North Pacific and Gulf of California

Hiroaki Yamagishi,[1,2,3,4] Marian B. Westley,[5,6] Brian N. Popp,[7] Sakae Toyoda,[2,8] Naohiro Yoshida,[1,2,3,8,9] Shuichi Watanabe,[1,2,10] Keisuke Koba,[1,2,11] and Yasuhiro Yamanaka[12,13]

Received 16 May 2006; revised 23 November 2006; accepted 22 December 2006; published 4 May 2007.

[1] Nitrous oxide (N_2O) is an important atmospheric greenhouse gas and is involved in stratospheric ozone depletion. Analysis of the isotopomer ratios of N_2O (i.e., the intramolecular distribution of ^{15}N within the linear NNO molecule and the conventional N and O isotope ratios) can elucidate the mechanisms of N_2O production and destruction. We analyzed the isotopomer ratios of dissolved N_2O at a site in the eastern tropical North Pacific (ETNP) and a site in the Gulf of California (GOC). At these sites, the flux of N_2O to the atmosphere is extremely high but denitrification activity in the oxygen minimum zone (OMZ) also reduces N_2O to N_2. We estimated the isotopomeric enrichment factors for N_2O reduction by denitrification. The factor was -11.6 ± 1.0‰ for the bulk (average) N, -19.8 ± 2.3‰ for the center N (α-site nitrogen), -3.4 ± 0.3‰ for the end N (β-site nitrogen), and -30.5 ± 3.2‰ for the ^{18}O of N_2O. Isotopomer analysis of N_2O suggests that nitrifiers should contribute to N_2O production more than denitrifiers at the oxycline above the OMZs in the ETNP (50–80 m) and in the GOC (80–300 m). In contrast, denitrifiers should largely contribute to the N_2O production and consumption in the OMZs both in the ETNP (120–130 m) and in the GOC (600–800 m). The N_2O isotopomer analysis will be a useful tool for resolving the distribution of water masses that carry a signal of N loss by denitrification.

Citation: Yamagishi, H., M. B. Westley, B. N. Popp, S. Toyoda, N. Yoshida, S. Watanabe, K. Koba, and Y. Yamanaka (2007), Role of nitrification and denitrification on the nitrous oxide cycle in the eastern tropical North Pacific and Gulf of California, *J. Geophys. Res.*, *112*, G02015, doi:10.1029/2006JG000227.

[1]Department of Environmental Science and Technology, Interdisciplinary Graduate School of Science and Engineering, Tokyo Institute of Technology, Yokohama, Japan.
[2]SORST Project, Japan Science and Technology Agency (JST), Kawaguchi, Japan.
[3]Research Center for the Evolving Earth and Planets, Tokyo Institute of Technology, Okayama, Japan.
[4]Now at Atmospheric Environmental Division, National Institute for Environmental Studies, Tsukuba, Japan.
[5]Department of Oceanography, School of Ocean and Earth Science and Technology, University of Hawaii, Honolulu, Hawaii, USA.
[6]Now at Geophysical Fluid Dynamics Laboratory, National Oceanic and Atmospheric Administration, Princeton, New Jersey, USA.
[7]Department of Geology and Geophysics, School of Ocean and Earth Science and Technology, University of Hawaii, Honolulu, Hawaii, USA.
[8]Department of Environmental Chemistry and Engineering, Interdisciplinary Graduate School of Science and Engineering, Tokyo Institute of Technology, Yokohama, Japan.
[9]Frontier Collaborative Research Center, Tokyo Institute of Technology, Yokohama, Japan.
[10]Mutsu Institute for Oceanography, Japan Agency for Marine-Earth Science and Technology, Mutsu, Japan.
[11]Now at Institute of Symbiotic Science and Technology, Tokyo University of Agriculture and Technology, Tokyo, Japan.
[12]Faculty of Environmental Earth Science, Hokkaido University, Sapporo, Japan.
[13]Frontier Research Center for Global Change, Japan Agency for Marine-Earth Science and Technology, Yokohama, Japan.

0148-0227/07/2006JG000227$09.00

1. Introduction

[2] Nitrous oxide (N_2O) is an important greenhouse gas [*Ramanathan et al.*, 1985], and also plays a role in stratospheric ozone chemistry [*Crutzen*, 1970]. The ocean is an important source of N_2O to the atmosphere; however estimates of its annual emission vary widely, for example, 3.0 ± 2 TgN [*Intergovernmental Panel on Climate Change*, 2001] (17% of the total emission) and 5.8 ± 2 TgN [*Nevison et al.*, 2003] (33% of the total emission), because observations are limited and models of the oceanic N_2O cycle are still evolving. Nitrification and denitrification are the main processes affecting the N_2O cycle in the oceans [*Suntharalingam and Sarmiento*, 2000]. Under aerobic conditions, N_2O is thought to be produced by autotrophic nitrifiers by chemical decomposition of hydroxylamine or of an intermediate between hydroxylamine and nitrite. Under low–oxygen conditions, N_2O production by autotrophic nitrifiers is enhanced, because ammonia oxidation to nitrite is accompanied by reduction of nitrite to N_2O [*Poth and Focht*, 1985; *Ritchie and Nicholas*, 1972], a process called nitrifier denitrification [*Poth and Focht*, 1985; *Wrage et al.*, 2001].

[3] The eastern tropical North Pacific (ETNP) is one of the three major low-oxygen regions of the world's ocean, which account for most of the world's water column denitrification [*Gruber and Sarmiento*, 1997]. Annual

N_2O emission is high from such low-oxygen regions [*Nevison et al.*, 1995], and has been estimated to be 25–50% of the total oceanic emission [*Suntharalingam et al.*, 2000]. Short-term fluctuations between a nondenitrification mode and a denitrification mode in the ETNP and the Arabian Sea could impact global climate by changes in N_2O emission [*Suthhof et al.*, 2001]. Therefore, in order to predict future changes in atmospheric N_2O concentration and to understand the impact of N_2O on climate, it is essential to understand the N_2O cycle in these low-oxygen regions in the oceans.

[4] The production processes of N_2O have been the subject of study for many years. *Cohen and Gordon* [1978] measured N_2O concentration in the ETNP and suggested that N_2O is produced by nitrification and consumed by denitrification on the basis of the correlation between N_2O concentration and apparent oxygen utilization (AOU) and the inverse correlation between N_2O concentration and nitrate deficit. In contrast, *Pierotti and Rasmussen* [1980] suggested that denitrification acts as a net source of N_2O under oxygen concentration of 0.1–0.3 mL L^{-1}, which is equivalent to 4.6–13.7 μmol kg^{-1} O_2 when sigmaθ is 26. *Yoshida et al.* [1984] suggested that the nitrogen isotope ratio of N_2O in the ETNP indicates that subsurface water is a source of N_2O and that the extremely oxygen-depleted water is a sink. *Yoshinari et al.* [1997] analyzed nitrogen and oxygen isotope ratios of N_2O in the oxic/suboxic boundaries in the ETNP and the Arabian Sea, and suggested that dissolved N_2O is enriched in ^{15}N and ^{18}O owing to N_2O reduction ($N_2O \rightarrow N_2$) by denitrification and could be an important source of atmospheric N_2O enriched in ^{15}N relative to tropospheric N_2O. On the basis of the concentrations of nutrients and the bulk nitrogen and oxygen isotope ratios of N_2O in the ETNP, *Westley et al.* [2001] suggested that N_2O at the concentration maximum is produced by nitrification within the subsurface oxycline whereas denitrification consumes N_2O in the core of the oxygen minimum zone (OMZ). However, the roles of microbial processes responsible for N_2O production have not been resolved sufficiently, in part owing to a lack of adequate analytical tools.

[5] Recently, techniques have been developed to measure the isotopomer ratios of N_2O (intramolecular distribution of ^{15}N within the linear NNO molecule) [*Toyoda and Yoshida*, 1999; *Brenninkmeijer and Röckmann*, 1999]. *Toyoda and Yoshida* [1999] defined the center and end positions of the N_2O molecule as α and β nitrogen, respectively, and the difference in isotope ratios between α and β-site nitrogen as the "^{15}N-site preference" ($SP = \delta^{15}N^{\alpha} - \delta^{15}N^{\beta}$). Isotopomer analysis of N_2O has been an important tool for resolving the N_2O cycle in the oceans. For example, in the subtropical North Pacific gyre, the minima o f $\delta^{15}N$ and $\delta^{18}O$ indicated subsurface production of N_2O and accounted for more than 40% of its emission from the surface to the atmosphere [*Dore et al.*, 1998]. Subsequent isotopomer analysis of N_2O constrained the ratio to 40–75% and moreover suggested that nitrification (via nitrifier-denitrification) accounted for the in situ N_2O production [*Popp et al.*, 2002].

[6] For relating isotopomer measurements to the production and consumption processes of N_2O, isotopomeric enrichment factors are essential. Recently, isotopomeric enrichment factors for N_2O production by nitrifiers [*Sutka et al.*, 2003, 2004a] and denitrifiers [*Sutka et al.*, 2006; *Toyoda et al.*, 2005] have been studied. However, there are few reports on the isotopomeric enrichment factor for N_2O reduction by denitrifiers, which is necessary in order to use N_2O isotopomer ratios quantitatively. Thus the objectives of this research are, first, to estimate the isotopomeric enrichment factor for N_2O reduction and, second, to resolve quantitatively production and consumption processes of nitrous oxide in the ETNP and Gulf of California (GOC) using N_2O isotopomer analysis.

[7] Here we estimated the isotopomeric enrichment factor for N_2O reduction in the core of the oxygen minimum zone in the ETNP. Applying this enrichment factor in a steady state model for the N_2O release from denitrifiers, we evaluated the contribution of each production process to the N_2O cycle in the ETNP and GOC. The isotopomer analysis suggests that nitrifiers play a more important role for N_2O production than denitrifiers in the subsurface layers, whereas denitrifiers produce and consume N_2O at the oxygen levels below about 1 μmol kg^{-1} in the upper and lower portions of the OMZs. We found that the SP of N_2O is a useful tool for resolving the N_2O cycle under the suboxic conditions in the oceans (Here we defined suboxic condition as $1 \leq [O_2] < 50$ μmol kg^{-1}).

2. Methods

2.1. Sampling

[8] Samples were collected in the ETNP (16°N, 107°W) at a site located in the core of the low-oxygen region during May–June 2000 on the R/V *Revelle*. The site is the same as Station 5 of the Eastern Pacific Redox Experiment (EPREX) research cruise [*Sansone et al.*, 2001; *Sutka et al.*, 2004b; *Westley et al.*, 2001]. Samples were also collected in the central GOC (26.30°N, 110.13°W) during September 2001 on the R/V *New Horizon*. The oxygen concentration was determined by Winkler titration [*Grasshoff et al.*, 1983]. Nitrite and ammonium were measured using colorimetry [*Grasshoff et al.*, 1983] and the fluorescence method of *Jones* [1991], respectively. Samples for N_2O concentration and isotopomer ratios were collected in 250-mL glass serum vials, preserved with $HgCl_2$, and sealed with butyl rubber stoppers (see *Popp et al.* [2002] for details).

2.2. N_2O Isotopomer Analysis

[9] For isotopomeric analysis, seawater was transferred from a serum vial to a sparging column and sparged with ultrapure helium (purity > 99.99995%). Water vapor and CO_2 were removed by magnesium perchlorate and NaOH (Ascarite II, GL Sciences Inc., Tokyo, Japan), respectively, and then extracted gases were collected on a stainless steel trap immersed in liquid nitrogen. These gases were carried by helium through Ascarite II and magnesium perchlorate again, and then cryofocused. N_2O was purified using a PoraPLOT-Q capillary column (25 m, 0.32 mm i.d., df = 10 μm, Varian, Inc., Palo Alto, USA) at 27°C. The N_2O isotopomer ratios were determined by duplicate measurements on a Finnigan MAT 252 with modified collectors (Thermo electron corporation, Bremen, Germany). First the ratios of δ(45/44) and δ(46/44) and the N_2O concentration

were measured by monitoring mass (m/z) 44, 45, and 46 ions simultaneously. Then the ratio of δ(31/30) was measured by monitoring mass (m/z) 30 and 31 fragment ions. For the analysis of δ(31/30), samples were further purified using a precolumn inserted after the preconcentration trap in order to remove an interfering substance detected in mass (m/z) 31. The substance is most likely a fluorocarbon (m/z 31 from CF^+) [*Kaiser et al.*, 2003]. The precolumn is a 1/4 inch o.d., 150-cm-long s.s. tube packed with silica gel (80/100 mesh) [*Toyoda et al.*, 2005]. The final isotopomer ratios were calculated following *Toyoda and Yoshida* [1999]. We adopted the definition of *Toyoda and Yoshida* [1999] for the isotopomer/isotope ratios of N_2O, namely $\delta^{15}N^{\alpha}$, $\delta^{15}N^{\beta}$, $\delta^{15}N^{bulk}$ (conventional $\delta^{15}N$), and $\delta^{18}O$. Isotopomer ratios of N_2O were calibrated with a standard gas produced by thermal decomposition of NH_4NO_3 [*Toyoda and Yoshida*, 1999]. The precision was estimated on the basis of the measurement of a laboratory reference gas dissolved in pure water to be less than ±0.2‰ for $\delta^{15}N^{bulk}$, ±0.4‰ for $\delta^{15}N^{\alpha}$, ±0.5‰ for $\delta^{15}N^{\beta}$, ±0.4‰ for $\delta^{18}O$, and ±0.9‰ for SP (1σ) of dissolved N_2O in duplicate 100 mL samples containing more than 20 nmol kg^{-1} N_2O. Equilibrium concentration of N_2O is calculated from potential temperature and salinity using the equation of *Weiss and Price* [1980].

2.3. Advection-Diffusion-Reaction Model

[10] We estimated the isotopomeric enrichment factors for N_2O reduction from the concentration and isotopomer ratios of N_2O at the ETNP site using one-dimensional, vertical advection-diffusion-reaction models containing one reaction. Assuming steady state and that the vertical diffusion coefficient (K) is independent of depth, we obtain the following differential equation:

$$K\left(\partial^2 N/\partial z^2\right) - V(\partial N/\partial z) - F_z = 0, \tag{1}$$

where K and V are the diffusion coefficient and advection velocity, respectively, in the z direction. The concentration and reduction rate of nitrous oxide are denoted by N and F_z, respectively. The values of each parameter are described in the Appendix. Assuming that N_2O reduction by denitrifiers can be a pseudo-first-order reaction of N_2O with the N_2O reduction rate (F_z) proportional only to the concentration of N_2O, the rate F_z is described as follows:

$$F_z = mN, \tag{2}$$

where, m is a reaction rate constant for the concentration model (validation of this assumption is discussed in section 4.2 and section I of auxiliary material Text S1[1]). The differential operators in equation (1) were replaced by the Euler method of forward-difference approximations. The detailed procedure for estimating enrichment factors follows the model of *Cline and Kaplan* [1975]. In the models, the step interval was set to 5 m. Fitting the model to the measured N_2O concentration gives N_2O reduction rates at each depth.

[11] In our model, we designate N_2O isotope or isotopomer ratios with δ_i:

$$\delta_i(‰) = \left(R_{i\text{-}sample}/R_{i\text{-}std} - 1\right) \times 1000 \tag{3}$$

where δ_i is $\delta^{15}N^{bulk}$, $\delta^{18}O$, $\delta^{15}N^{\alpha}$, or $\delta^{15}N^{\beta}$, and std is a standard. R_i is $^{15}R^{bulk}$, ^{18}R, $^{15}R^{\alpha}$, or $^{15}R^{\beta}$, respectively, which are $\{[^{14}N^{15}N^{16}O] + [^{15}N^{14}N^{16}O]\}/2$ $[^{14}N^{14}N^{16}O]$, $[^{14}N^{14}N^{18}O]/[^{14}N^{14}N^{16}O]$, $[^{14}N^{15}N^{16}O]/[^{14}N^{14}N^{16}O]$, or $[^{15}N^{14}N^{16}O]/[^{14}N^{14}N^{16}O]$, respectively. The fractionation factors (α_i) are defined following *Mariotti et al.* [1981],

$$\alpha_i \equiv m/m, \tag{4}$$

where m is a reaction rate constant of the most abundant isotopomer, namely, $^{14}N^{14}N^{16}O$, for N_2O reduction, i describes bulk-N, ^{18}O, α, or β, and m_i are reaction rate constants for either ^{15}N- or ^{18}O-isotopes, or either $^{14}N^{15}N^{16}O$- ($^{15}N^{\alpha}$-) or $^{15}N^{14}N^{16}O$- ($^{15}N^{\beta}$-) isotopomers, respectively. Enrichment factors (ε_i) are defined following *Mariotti et al.* [1981],

$$\varepsilon_i \equiv (\alpha_i - 1) \times 1000. \tag{5}$$

[12] This definition gives a negative value for an isotopic/isotopomeric enrichment factor, which is used in some reports [*Mariotti et al.*, 1981; *Ostrom et al.*, 2002]. The benefit of the definition is that it gives consistency between the value of the site preference of produced N_2O and the isotopomeric enrichment factors for decomposition of N_2O (see section II of auxiliary material Text S1). Substituting the concentrations of ^{15}N- and ^{18}O-isotopes, and $^{15}N^{\alpha}$- and $^{15}N^{\beta}$-isotopomers into equation (1), and using the definitions of δ_i and α_i from equations (3) and (4), we obtain equation (6) for the isotopomer model,

$$K(N\delta_i)'' - V(N\delta_i)' - 1000m_i(\alpha_i - 1)N - m_i\alpha_i(N\delta_i) = 0, \tag{6}$$

where the primes refer to successive differentiation with respect to depth. The differential operators in equation 6 were replaced by the Euler method of forward-difference approximations [*Cline and Kaplan*, 1975]. The isotopomeric enrichment factors were estimated by fitting the models to the observed isotopomer ratios.

2.4. Interpreting Origins of N_2O From Isotopomer Analysis

[13] When interpreting N_2O isotopomer ratios of ($\delta^{15}N^{\alpha}$, $\delta^{15}N^{\beta}$, $\delta^{18}O$) quantitatively, it is reasonable to use isotopomeric enrichment factors of (ε_{α}, ε_{β}, ε_{18O}). However, quantitative analysis of $\delta^{18}O$-N_2O is difficult because oxygen in a substrate, nitrite, can exchange with that in water during denitrification [*Casciotti et al.*, 2002; *Shearer and Kohl*, 1988], and moreover there are no data on the isotope composition of O_2 in the ETNP and GOC sites and of $\delta^{18}O$ of nitrate in the GOC. On the other hand, the site preference of N_2O is considered to be independent of the isotope ratios of the substrate during N_2O production by nitrifiers and denitrifiers because the SP of N_2O produced by nitrifiers [*Sutka et al.*, 2003] and denitrifiers [*Toyoda et al.*, 2005] is nearly constant even if the $\delta^{15}N^{bulk}$ and $\delta^{18}O$ of N_2O are changed owing to the increase of the isotope ratios

[1] Auxiliary material data sets are available at ftp://ftp.agu.org/apend/jg/2006jg000227. Other auxiliary material files are in the HTML.

of residual substrates. Considering that SP of N_2O should not be influenced by the isotope ratio of its substrates and that $\delta^{15}N^{bulk}$ of N_2O can be interpreted using enrichment factors of bulk nitrogen, analyzing N_2O on a plot of SP versus $\delta^{15}N^{bulk}$ should have more benefit than on a plot of $\delta^{15}N^{\alpha}$ versus $\delta^{15}N^{\beta}$.

[14] Thus we demonstrate the validity of the analysis of isotopomer fractionation of N_2O reduction on the plot of SP versus $\delta^{15}N^{bulk}$ (see section II of auxiliary material Text S1 for details) and then we analyze the production processes of N_2O in the ETNP and GOC on a plot of SP versus $\delta^{15}N^{bulk}$. In the case of a one step reaction (substrate → product), we define apparent isotopomeric fractionation factors of α-site or β-site nitrogens in N_2O following *Mariotti et al.* [1981],

$$\alpha_\alpha \equiv \left(\frac{{}^{15}R_p^\alpha}{{}^{15}R_s^\alpha}\right) \tag{7a}$$

$$\alpha_\beta \equiv \left(\frac{{}^{15}R_p^\beta}{{}^{15}R_s^\beta}\right), \tag{7b}$$

where subscripts of p and s are product and substrate, respectively. When equations (3) and (5) are inserted into equations (7a) and (7b), and then the logarithm is taken, the following equations are obtained:

$$\ln\left(1+\frac{\varepsilon_\alpha}{1000}\right) = \ln\left(1+\frac{\delta^{15}N_p^\alpha}{1000}\right) - \ln\left(1+\frac{\delta^{15}N_s^\alpha}{1000}\right) \tag{8}$$

$$\ln\left(1+\frac{\varepsilon_\beta}{1000}\right) = \ln\left(1+\frac{\delta^{15}N_p^\beta}{1000}\right) - \ln\left(1+\frac{\delta^{15}N_s^\beta}{1000}\right). \tag{9}$$

We define the isotopomeric enrichment factor for SP in N_2O as $\varepsilon_{SP} \equiv \varepsilon_\alpha - \varepsilon_\beta$. When the following conditions (equation (10)) can be applied, equations (8) and (9) can be combined to give equation (11),

$$\frac{\varepsilon_\alpha}{1000}, \frac{\varepsilon_\beta}{1000}, \frac{\delta^{15}N_p^\alpha}{1000}, \frac{\delta^{15}N_p^\beta}{1000}, \frac{\delta^{15}N_s^\alpha}{1000}, and \frac{\delta^{15}N_s^\beta}{1000} \ll 1 \tag{10}$$

$$SP_p \approx SP_s + \varepsilon_{SP}. \tag{11}$$

Therefore a plot of SP versus $\delta^{15}N^{bulk}$ can be substituted for a plot of $\delta^{15}N^{\alpha}$ versus $\delta^{15}N^{\beta}$ during the analysis of isotopomer effect for N_2O production and consumption.

[15] Since N_2O is an intermediate of denitrification, the isotopomer ratios of N_2O inside the cell of denitrifiers and N_2O dissolved in the water column should be different. Here we designate N_2O inside denitrifiers and in the water column as N_2O_{vivo} and N_2O_{situ}, respectively. Assuming that the flux of N_2O released from the cells of denitrifiers during denitrification (the flux from N_2O_{vivo} to N_2O_{situ}) and the consumption flux of dissolved N_2O (the flux from N_2O_{situ} to N_2O_{vivo}) are negligible compared with the rate of denitrification (the fluxes from NO_3^- to N_2O_{vivo} and N_2O_{vivo} to N_2), isotopomer ratios of N_2O released from the cell of denitrifiers can be calculated [*Barford et al.*, 1999]. The N_2O isotopomer ratios should be controlled by production and reduction processes as follows:

$$\boldsymbol{\delta}\text{-}NO_3^- \xrightarrow{\varepsilon_{NaR},\boldsymbol{\delta}\text{-}N_2O_{D\text{-}pro}} \boldsymbol{\delta}\text{-}N_2O_{D\text{-}rel} \xrightarrow{\varepsilon_{N2OR},\boldsymbol{\delta}\text{-}N_{2D\text{-}pro}} \boldsymbol{\delta}\text{-}N_2, \tag{12}$$

where the bold italic symbols of $\boldsymbol{\varepsilon}$ and $\boldsymbol{\delta}$ indicate the matrices of ($\boldsymbol{\delta}^{15}N^{bulk}$, SP). The SP of $\boldsymbol{\delta}$-NO_3^- is recognized as zero for convenience. The symbols of ε_{NaR} and ε_{N2OR} indicate the isotopomeric enrichment factors for nitrate reduction to N_2O and for N_2O reduction to N_2, respectively. The instantaneous products of N_2O and N_2 are expressed as $\boldsymbol{\delta}$-$N_2O_{D\text{-}pro}$ and $\boldsymbol{\delta}$-$N_{2D\text{-}pro}$, respectively. *Barford et al.* [1999] suggest the following correlations under steady state:

$$\varepsilon_{NaR} = \boldsymbol{\delta}\text{-}N_2O_{D\text{-}pro} - \boldsymbol{\delta}\text{-}NO_3^-, \tag{13}$$

$$\varepsilon_{N2OR} = \boldsymbol{\delta}\text{-}N_{2D\text{-}pro} - \boldsymbol{\delta}\text{-}N_2O_{D\text{-}rel}, \tag{14}$$

$$\boldsymbol{\delta}\text{-}N_{2D\text{-}pro} = \boldsymbol{\delta}\text{-}N_2O_{D\text{-}pro}. \tag{15}$$

Isotopomer ratios of N_2O produced by denitrifiers ($\boldsymbol{\delta}$-$N_2O_{D\text{-}pro}$) and N_2O released from denitrifiers ($\boldsymbol{\delta}$-$N_2O_{D\text{-}rel}$) are calculated from equations (13), (14), and (15) as follows:

$$\boldsymbol{\delta}\text{-}N_2O_{D\text{-}pro} = \boldsymbol{\delta}\text{-}NO_3^- + \varepsilon_{NaR} \tag{16}$$

$$\boldsymbol{\delta}\text{-}N_2O_{D\text{-}rel} = \boldsymbol{\delta}\text{-}N_2O_{D\text{-}pro} - \varepsilon_{N2OR}. \tag{17}$$

N_2O is released by nitrifiers and denitrifiers, and simultaneously dissolved N_2O is consumed by denitrifiers, therefore the isotopomer ratios of dissolved N_2O ($\boldsymbol{\delta}$-N_2O_{situ}) can be written as follows:

$$\boldsymbol{\delta}\text{-}N_2O_{situ} = t\boldsymbol{\delta}\text{-}N_2O_{N\text{-}pro} + (1-t)\boldsymbol{\delta}\text{-}N_2O_{D\text{-}rel} - \nu\varepsilon_{N2OR}, \tag{18}$$

where t ($0 \le t \le 1$) is the ratio of the N_2O released from nitrifiers to the total N_2O released into the water column (abbreviated as N-ratio), $\boldsymbol{\delta}$-$N_2O_{N\text{-}pro}$ represents the isotopomer ratios of N_2O produced by nitrifiers, and ν is an arbitrary positive quantity. Because the parameters of $\boldsymbol{\delta}$-N_2O_{situ}, $\boldsymbol{\delta}$-$N_2O_{N\text{-}pro}$, $\boldsymbol{\delta}$-$N_2O_{D\text{-}rel}$, and ε_{N2OR} are the matrixes of $\delta^{15}N^{bulk}$ and SP ($\delta^{15}N^{bulk}$, SP), ratios of N_2O released from nitrifiers and denitrifiers can be estimated on the basis of plots of SP versus $\delta^{15}N^{bulk}$ (Figure 1). The ratio t is estimated following equation (19) (see section III of auxiliary material Text S1 for the derivation of equation (19)).

$$t = \{(y_1 - y_3) - a(x_1 - x_3)\}/\{(y_1 - y_2) - a(x_1 - x_2)\}, \tag{19}$$

where each plot is defined as follows: $\boldsymbol{\delta}$-$N_2O_{D\text{-}rel}$ (x_1, y_1), $\boldsymbol{\delta}$-$N_2O_{N\text{-}pro}$ (x_2, y_2), and $\boldsymbol{\delta}$-N_2O_{situ} (x_3, y_3). The constant, a, is equivalent to the slope of the regression line for N_2O reduction on the SP-$\delta^{15}N^{bluk}$ plot. The error of the ratio t is estimated following propagation of errors in equation (19)

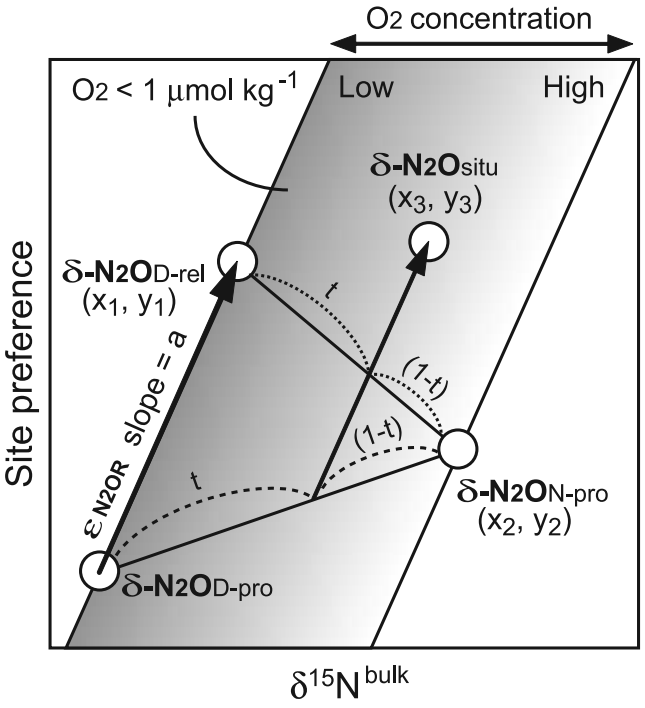

Figure 1. Plots of the site preference (SP) versus $\delta^{15}N^{bulk}$ of N_2O for estimating the contribution of nitrification and denitrification as the production processes of N_2O. The t is the ratio of N_2O released from nitrifiers to the total N_2O released from both nitrifiers and denitrifiers. Each notation is defined in text (section 2.4).

using a = 1.43 ± 0.14, which was estimated from the regression line over the depth range 400–700 m at the ETNP site.

3. Results

[16] The N_2O concentration maximum (85 nmol kg^{-1}) in the ETNP was found at the depth of 65–85 m in the oxycline (Figure 2a). Below 85 m, N_2O concentration decreased rapidly to 7.8 nmol kg^{-1} (130 m), which is below the equilibrium concentration. The O_2 concentration was <1.5 μmol kg^{-1} O_2 below 100 m (Table 1). A secondary N_2O concentration maximum (56.5 nmol kg^{-1}) was observed at 800 m under suboxic conditions (2.7 μmol kg^{-1} O_2). These features are consistent with previous observations in the ETNP [*Cohen and Gordon*, 1978; *Nevison et al.*, 2003; *Pierotti and Rasmussen*, 1980; *Yoshinari et al.*, 1997].

[17] N_2O production is enhanced under suboxic conditions; thus N_2O should be produced at the oxycline around 75 m, where the N_2O concentration maximum formed a sharp peak in the N_2O concentration profile at the ETNP site. Potential temperature and salinity at the depth of 50–75 m plot linearly on a T-S diagram, which indicates the mixing of two water masses. Thus N_2O produced at the oxycline should diffuse to the mixed layer by vertical mixing and then be released to the troposphere by air-sea gas exchange. N_2O isotopomer ratios at the surface were similar to those of the troposphere (Figure 2b), which indicates that N_2O in the troposphere should be dissolved at least in the mixed layer. Assuming that the N_2O profile from the N_2O concentration maximum to the surface is formed by mixing of the background tropospheric N_2O and the N_2O produced at the oxycline, we can use a Keeling Plot, a plot of isotope ratios versus the reciprocal N_2O concentration (Figure 3), to estimate the isotopomer ratios of N_2O produced at the oxycline. Intercepts of regression lines estimate isotopomer ratios of a produced substance [*Pataki et al.*, 2003].

[18] The isotopomer ratios of N_2O produced at the subsurface N_2O maximum in the ETNP were 3.2 ± 0.1, 8.7 ± 0.6, −2.3 ± 0.6, 47.6 ± 0.3, and 11.0 ± 1.2‰, for $\delta^{15}N^{bulk}$, $\delta^{15}N^{\alpha}$, $\delta^{15}N^{\beta}$, $\delta^{18}O$, and the site preference, respectively (1σ, n = 5). The $\delta^{15}N^{bulk}$ and $\delta^{18}O$ estimates are similar to the measured subsurface values in the ETNP ($\delta^{15}N^{bulk}$ = 5 ± 2‰ and $\delta^{18}O_{VSMOW}$ = 50 ± 2‰ [*Yoshinari et al.*, 1997]) and the Arabian Sea ($\delta^{15}N^{bulk}$ = 7 ± 2‰ and $\delta^{18}O_{VSMOW}$ = 49 ± 2‰ [*Yoshinari et al.*, 1997]; $\delta^{15}N^{bulk}$ = 2 ± 2‰ and $\delta^{18}O_{VSMOW}$ = 47 ± 6‰ [*Naqvi et al.*, 1998]). The $\delta^{15}N^{bulk}$ estimate is also similar to the $\delta^{15}N^{bulk}$ estimated from Keeling Plots in the subtropical gyre ($\delta^{15}N^{bulk}$ = 3.7‰ [*Popp et al.*, 2002]). The remarkable consistency of the isotope ratios of N_2O strongly suggests that the production process is similar in the subsurface layer despite the large disparity in geographic regions. The consistent $\delta^{15}N$ values of the y-intercept of the Keeling Plot for such a wide range of oceanic environments is startling and further suggests uniformity in the processes that form N_2O in oceanic surface waters.

[19] At the GOC site, the suboxic interface was located at about 300 m (Figure 2d) and the N_2O concentration was highest at 700 m, well within the oxygen minimum zone (O_2< 1 μmol kg^{-1}). At 700 m, site preference was high, whereas $\delta^{15}N^{bulk}$ and $\delta^{18}O$ were low, relative to those of N_2O at the suboxic interface (300 m; see Figure 2e). Incubation of sediments indicates that the dominant source of N_2O is denitrification at oxygen levels <1 μmol kg^{-1} [*Jørgensen et al.* [1984]. Considering the low O_2 concentration (<1 μmol kg^{-1}) and the negative N* (Figure 2f), which is an indicator for nitrate deficit (N* = $[NO_3^-]$ − 16 $[PO_4^{3-}]$ + 2.90 μmol kg^{-1} [*Deutsch et al.*, 2001]), denitrification should be the primary source of N_2O at 700 m.

4. Discussion

4.1. Nitrous Oxide Cycle in the Oxygen Minimum Zone of the ETNP

[20] At oxygen levels below 1 μmol kg^{-1}, the consumption of N_2O by denitrification becomes the dominant process and drives N_2O concentrations below equilibrium concentrations [*Codispoti et al.*, 1992; *Prosperie et al.*, 1996; *Suntharalingam et al.*, 2000]. Actually, N_2O concentration was lower than its equilibrium concentration at the depth of 130–500 m at the ETNP site (Table 1 and Figure 2a), which indicates that N_2O reduction by denitrifiers is active. Therefore isotopomer ratios of N_2O should be affected by the isotope effect associated with N_2O reduction by denitrifiers.

[21] The $\delta^{15}N^{\alpha}$, $\delta^{15}N^{\beta}$ and $\delta^{15}N^{bulk}$ of N_2O are all linearly correlated with the $\delta^{18}O$ of N_2O from 400 to 700 m (Figure 4a). Strong linear correlation between these three

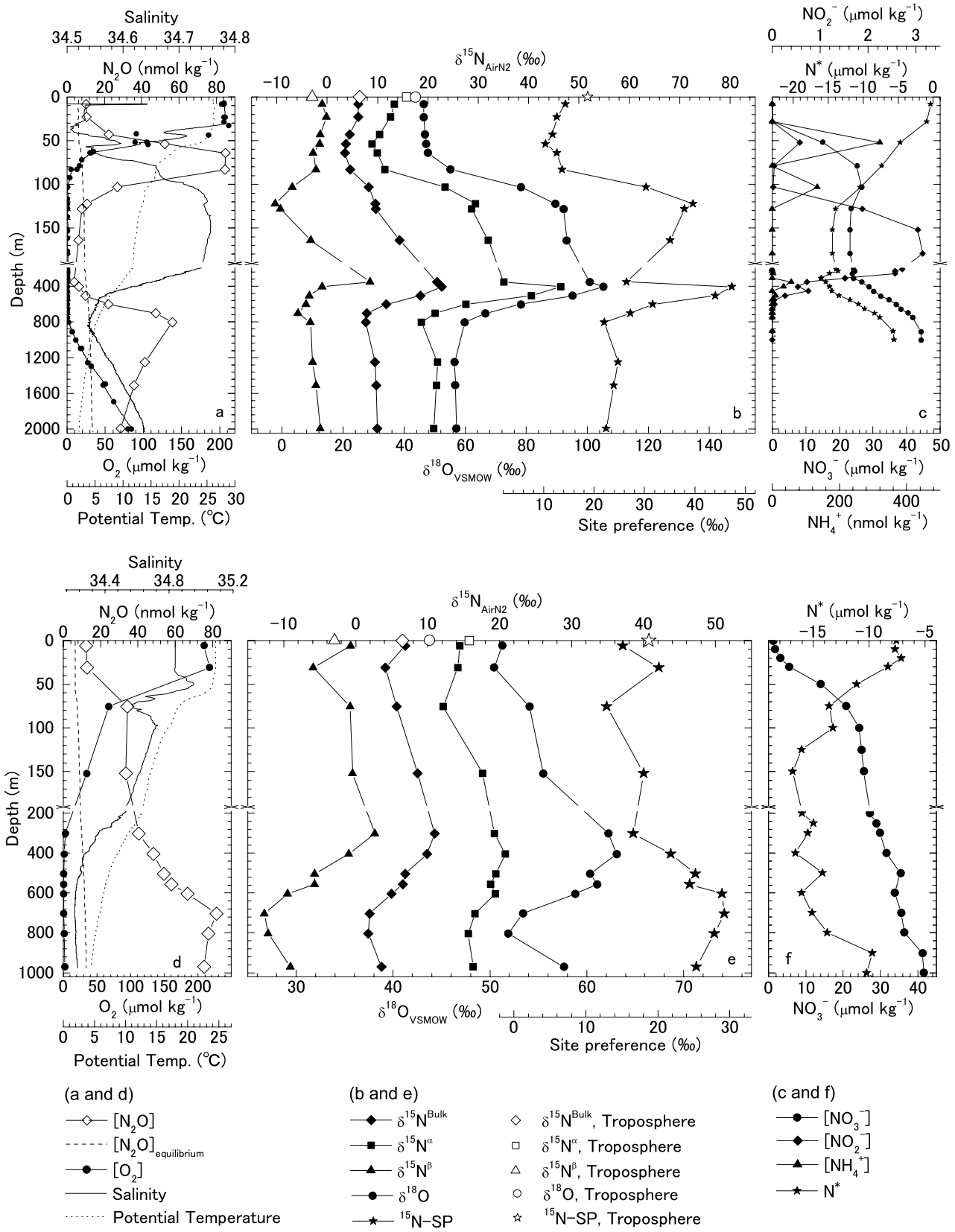
Salinity
34.5 34.6 34.7 34.8
N_2O (nmol kg^{-1})
0 20 40 60 80
Depth (m)
0 50 100 150 400 800 1200 1600 2000
a
0 50 100 150 200
O_2 (μmol kg^{-1})
0 5 10 15 20 25 30
Potential Temp. (°C)
$\delta^{15}N_{AirN2}$ (‰)
−10 0 10 20 30 40 50 60 70 80
b
0 20 40 60 80 100 120 140
$\delta^{18}O_{VSMOW}$ (‰)
10 20 30 40 50
Site preference (‰)
NO_2^- (μmol kg^{-1})
0 1 2 3
N^* (μmol kg^{-1})
−20 −15 −10 −5 0
c
0 10 20 30 40 50
NO_3^- (μmol kg^{-1})
0 200 400
NH_4^+ (nmol kg^{-1})
Salinity
34.4 34.8 35.2
N_2O (nmol kg^{-1})
0 20 40 60 80
Depth (m)
0 50 100 150 200 400 600 800 1000
d
0 50 100 150 200
O_2 (μmol kg^{-1})
0 5 10 15 20 25
Potential Temp. (°C)
$\delta^{15}N_{AirN2}$ (‰)
−10 0 10 20 30 40 50
e
30 40 50 60 70
$\delta^{18}O_{VSMOW}$ (‰)
0 10 20 30
Site preference (‰)
N^* (μmol kg^{-1})
−15 −10 −5
f
0 10 20 30 40
NO_3^- (μmol kg^{-1})
(a and d)
[N_2O]
[N_2O]$_{equilibrium}$
[O_2]
Salinity
Potential Temperature
(b and e)
$\delta^{15}N^{Bulk}$
$\delta^{15}N^{\alpha}$
$\delta^{15}N^{\beta}$
$\delta^{18}O$
^{15}N-SP
$\delta^{15}N^{Bulk}$, Troposphere
$\delta^{15}N^{\alpha}$, Troposphere
$\delta^{15}N^{\beta}$, Troposphere
$\delta^{18}O$, Troposphere
^{15}N-SP, Troposphere
(c and f)
[NO_3^-]
[NO_2^-]
[NH_4^+]
N^*

Figure 2

Table 1. Concentration and Isotopomer Ratios of N_2O in the Eastern Tropical North Pacific and Gulf of California

Depth, m	Sigmaθ	O_2, μmol kg^{-1}	N_2O, nmol kg^{-1}	Saturation,[a] %	$\delta^{15}N^{bulk}$, ‰	$\delta^{15}N^{\alpha}$, ‰	$\delta^{15}N^{\beta}$, ‰	$\delta^{18}O$, ‰	SP, ‰
Eastern Tropical North Pacific (16°N, 107°W)									
10	22.34	205.41	10.07	172	6.15	13.31	−1.02	46.45	14.33
25	22.42	205.49	10.37	177	6.23	12.56	−0.10	46.37	12.66
45	22.55	185.64	22.45	379	4.51	10.40	−1.38	46.87	11.78
55	23.48	105.94	52.37	810	3.75	8.92	−1.42	47.11	10.35
65	25.02	30.77	84.79	1099	3.60	9.93	−2.74	47.81	12.68
85	25.67	5.54	84.57	1009	4.62	11.44	−2.20	55.21	13.64
105	26.02	0.65	26.89	306	8.26	23.43	−6.91	78.19	30.34
120	26.12	1.41	10.58	119	9.58	29.43	−10.27	89.52	39.70
130	26.16	0.40	7.84	88	9.70	28.71	−9.30	92.26	38.01
165	26.38	0.47 [b]	6.10	66	14.37	31.96	−3.22	93.34	35.17
350	26.73	0.19	3.80	38	21.82	35.08	8.57	100.75	26.50
400	26.83	0.39	6.27	60	22.74	46.42	−0.95	105.30	47.37
500	26.96	0.76	9.82	91	18.50	40.56	−3.56	95.15	44.12
600	27.09	0.28	22.19	198	11.73	27.58	−4.12	78.19	31.70
700	27.19	0.45	47.48	411	7.85	21.47	−5.77	66.64	27.24
800	27.27	2.70	56.51	477	7.71	18.73	−3.30	59.97	22.03
1250	27.49	27.50	41.77	330	9.52	21.93	−2.89	56.51	24.82
1510	27.57	47.49	35.92	277	9.76	21.73	−2.20	56.88	23.93
1995	27.66	80.13	28.85	216	9.92	21.15	−1.32	57.06	22.47
Gulf of California (26.30°N, 110.13°W)									
5	23.38	208.81	12.19	194	6.90	14.47	−0.67	51.29	15.14
30	23.43	216.77	12.61	201	4.14	14.20	−5.92	50.42	20.12
75	24.79	67.88	34.40	459	5.70	12.15	−0.75	54.08	12.89
150	25.90	34.21	33.58	385	8.60	17.62	−0.41	55.52	18.03
300	26.38	3.05	40.54	411	10.97	19.26	2.68	62.21	16.58
405	26.59	1.22	48.20	460	9.90	20.78	−0.99	63.12	21.76
505	26.76	0.61	53.87	490	6.89	19.50	−5.72	60.34	25.23
555	26.83	0.61	58.04	517	6.55	18.78	−5.69	61.09	24.46
605	26.88	0.61	66.59	584	4.95	19.40	−9.49	58.81	28.88
705	26.94	0.61	82.17	706	1.94	16.55	−12.67	53.39	29.22
805	27.03	1.22	77.84	652	1.76	15.68	−12.17	51.88	27.85
970	27.12	2.44	75.40	614	3.62	16.30	−9.06	57.60	25.35

[a]Saturation (%) = $[N_2O]_{measured}/[N_2O]_{equilibrium} \times 100$. Equilibrated concentration was calculated following *Weiss and Price* [1980].
[b]Oxygen concentration was measured from a different cast with the cast of N_2O.

independent parameters ($\delta^{15}N^{bulk}$, $\delta^{18}O$, and SP) is strong evidence for either isotopomer fractionation associated with a one-step reaction or mixing of two different pools of N_2O. Since N_2O consumption is surely active at oxygen levels below 1 μmol kg^{-1} and mixing of waters by cross-isopycnal diffusion across 300 m is unlikely to account for the linear correlation, we suggest that the highly linear correlations between 400 and 700 m (Figure 4a) result from N_2O consumption by denitrification rather than by mixing between isotopically distinct pools of N_2O. The $\delta^{15}N^{bulk}$, $\delta^{15}N^{\alpha}$, $\delta^{18}O$, and SP of N_2O increased as N_2O concentration decreased, and the $\delta^{15}N^{\beta}$ slightly increased from 700 m to 400 m (Figures 2a and 2b). This correlation is consistent with kinetic isotope effects associated with the cleavage of the N-O bonds during N_2O reduction by denitrification [*Popp et al.*, 2002; *Toyoda et al.*, 2002; *Westley et al.*, 2006]. Therefore the concentration and isotopomer ratios of N_2O from 700 to 400 m suggest that the N_2O is produced in the suboxic zone (the area below 750 m, where $[O_2] \geq 1$ μmol kg^{-1}) and then diffuses and advects into the OMZ up to 400 m, which is the strongest anoxic zone at the ETNP site on the basis of ammonium accumulation (Figure 2c).

[22] Linear correlations between $\delta^{18}O$-N_2O and $\delta^{15}N^{\alpha}$-, $\delta^{15}N^{\beta}$-, or $\delta^{15}N^{bulk}$-N_2O were also observed over the depth range 65–130 m (Figure 4b). At 65 m, low $\delta^{15}N^{bulk}$, $\delta^{18}O$, and SP of N_2O relative to that in the troposphere can be attributed to the N_2O production under suboxic conditions. From 65 m to 130 m, oxygen concentration decreases with depth, which results in the shift of the N_2O production process from nitrification to denitrification, and the

Figure 2. Concentration and isotopomer ratios of N_2O and concentrations of O_2 and nitrogen compounds plotted versus depth in (a, b, c) the ETNP and (d, e, f) the Gulf of California. Figures 2a and 2d show N_2O concentration (open diamond), O_2 concentration (solid circle), equilibrium N_2O concentration (dashed line), salinity (solid line), and potential temperature (dotted line). Figures 2b and 2e show $\delta^{15}N^{bulk}$ (solid diamond), $\delta^{15}N^{\alpha}$ (solid square), $\delta^{15}N^{\beta}$ (solid triangle), $\delta^{18}O$ (solid circle), and ^{15}N-site preference (solid star) of dissolved N_2O; $\delta^{15}N^{bulk}$ (open diamond), $\delta^{15}N^{\alpha}$ (open square), $\delta^{15}N^{\beta}$ (open triangle), $\delta^{18}O$ (open circle), and ^{15}N-site preference (open star) of tropospheric N_2O [*Yoshida and Toyoda*, 2000]. Figures 2c and 2f show nitrate (solid circle), nitrite (solid diamond), and ammonia (solid triangle) concentrations, and N* (solid star). In Figure 2f, nitrate concentration and N* were calculated from the annual analyzed mean nutrient, salinity, and temperature at 26.5°N, 110.5°W [*Boyer et al.*, 2002; *Conkright et al.*, 2002; *Stephens et al.*, 2002]. All isotopic values are expressed as permil (‰) deviations from atmospheric N_2 (for nitrogen) and VSMOW (for oxygen). The equilibrium concentration of N_2O was calculated following *Weiss and Price* [1980].

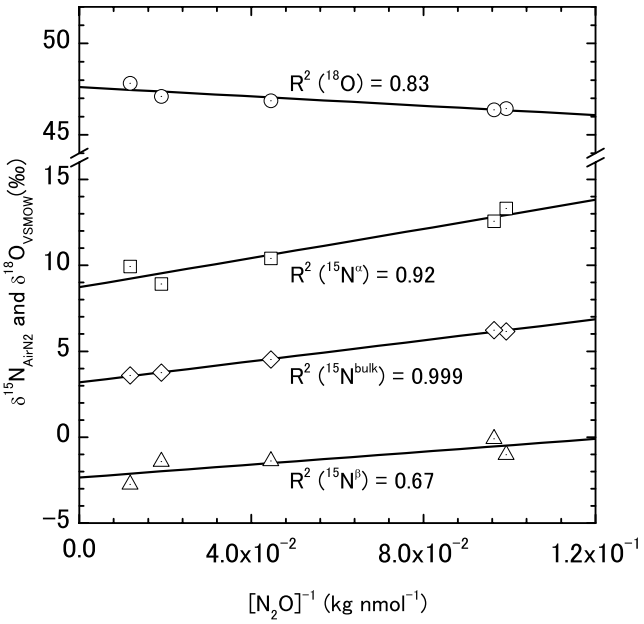

Figure 3. Isotopomer ratios of N_2O versus reciprocal N_2O concentration at the ETNP site (10–65 m). The value of intercept represents isotopomer ratio of a source (i.e., an end-member). The end-member equals the isotopomer ratios of N_2O produced at the concentration maximum. Each plot represents $\delta^{15}N^{bulk}$ (open diamond), $\delta^{15}N^{\alpha}$ (open square), $\delta^{15}N^{\beta}$ (open triangle), and $\delta^{18}O$ (open circle).

increase of the ratio of N_2O reduction to its production. This suggestion is consistent with the profile of N* (Figure 2c). The value of N* decreased as depth increased to 100 m, which suggests denitrification is active at least below the depth of 100 m. Over the depth range 65–130 m, $\delta^{15}N^{\beta}$-N_2O decreased with depth, which could be caused by production of N_2O with low $\delta^{15}N^{bulk}$ and subsequent consumption of dissolved N_2O. A decrease of $\delta^{15}N^{\beta}$ accompanied by increases of $\delta^{18}O$ and SP was also observed in the Black Sea [*Westley et al.*, 2006]. Therefore the correlation between $\delta^{18}O$-N_2O and $\delta^{15}N^{\alpha}$-, $\delta^{15}N^{\beta}$-, or $\delta^{15}N^{bulk}$-N_2O at 65–130 m should be the result of a shift in the production and consumption processes of N_2O. Potential temperature and salinity at 65–130 m follow a linear trend on a T-S diagram (data not shown), which indicates the mixing of two water masses. Therefore the good correlation between N_2O isotopomer ratios over the depth range 65 to 130 m could be attributed to mixing of water masses. (Correlation coefficient (R^2) is listed in the caption of Figure 4).

4.2. Isotopomeric Enrichment Factors for N_2O Reduction

[23] If in situ production or isopycnal diffusion affects the distribution of N_2O between 400 and 700 m at the ETNP site in addition to the in situ N_2O reduction, then N_2O isotopomer ratios should plot as curves in $\delta^{15}N$ versus $\delta^{18}O$ space. The observed linear correlation between N_2O isotopomer ratios between 400 and 700 m indicates that only one of these processes affects the N_2O pool. The OMZs in the ETNP are considered as stagnant layers ventilated only by mixing with surface and deep oxygenated waters [*Wyrtki*, 1962]. Actually, distribution of N* at Sigmaθ = 26.9 and 27.1, which are equivalent to $\sim$ 450 and 600 m, respectively [*Castro et al.*, 2001], indicates that the water mass at the ETNP site is stagnant and appears to be isolated from other water masses. Therefore it is reasonable to assume that only in situ N_2O reduction affects the pool of N_2O and to analyze the N_2O isotopomer ratios between 400 to 700 m using vertical advection-diffusion-reaction models.

[24] There are several factors that could control N_2O reduction rate, such as N_2O, O_2, or nitrate concentrations, or potential denitrification activity. Oxygen and nitrate can compete with N_2O as electron accepters. However, the oxygen concentration was under 1 μmol/kg from 400–700 m and showed no concentration gradients. Therefore it is not necessary to include O_2 concentration among the factors controlling N_2O reduction rate as a function of depth. Negative N* from 400–700 m indicates that nitrate is a competitor of N_2O over this depth interval (Figure 2c). The concentration of nitrate was approximately a thousand times higher than the N_2O concentration. Therefore N_2O concentration rather than nitrate concentration seems to constrain the N_2O reduction rate. During nitrate reduction, organic matter is thought to regulate the nitrate reduction

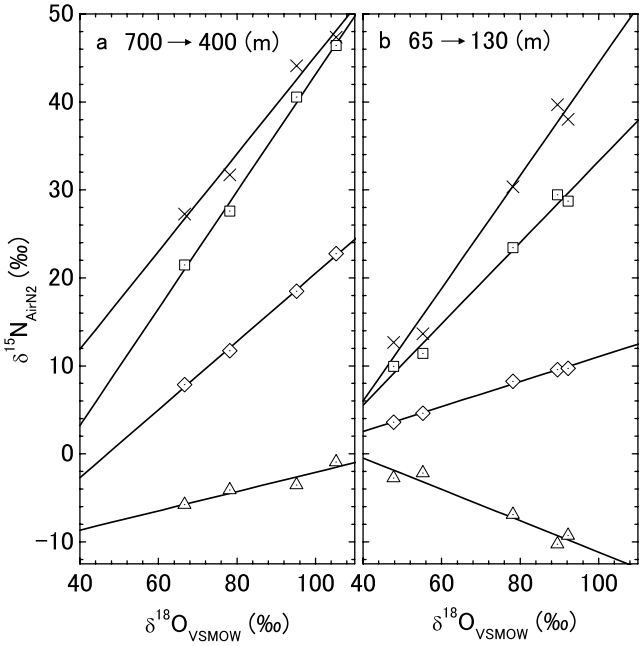

Figure 4. Relationship between nitrogen isotope/isotopomer ratios and oxygen isotope ratio of N_2O (a) between 400 and 700 m and (b) between 65 and 130 m at the ETNP site. Each plot represents $\delta^{15}N^{bulk}$ (open diamond), $\delta^{15}N^{\alpha}$ (open square), $\delta^{15}N^{\beta}$ (open triangle), and ^{15}N-site preference (cross). Regression lines of 400–700 m are as follows, where a cross denotes $\delta^{18}O$ and the value in parentheses is R^2 (n = 4): $\delta^{15}N^{bulk} = -18.21 + 0.387$ X (0.998), $\delta^{15}N^{\alpha} = -23.36 + 0.665$ X (0.995), $\delta^{15}N^{\beta} = -13.05 + 0.109$ X (0.890), and SP = $-10.31 + 0.555$ X (0.981). Regression lines of 65 – 130 m are as follows (n = 5): $\delta^{15}N^{bulk} = -3.14 + 0.142$ X (0.995), $\delta^{15}N^{\alpha} = -12.94 + 0.462$ X (0.989), $\delta^{15}N^{\beta} = 6.66 - 0.178$ X (0.944), and SP = $-19.60 + 0.640$ X (0.980).

rate because denitrification activity can be limited by the supply of electron donors (organic compounds) rather than electron accepters such as nitrate [*Cline and Kaplan*, 1975; *Sutka et al.*, 2004b]. However, considering that the nitrate reduction rate is likely at least 2 orders of magnitude higher than the N_2O reduction rate, it is probable that electron donors should be sufficient for N_2O reduction and that N_2O reduction can be a pseudo-first-order reaction of N_2O. Thus we developed the advection-diffusion-reaction model with the assumption that the N_2O reduction rate is only proportional to the concentration of N_2O (see section 2.3 for the description of the model). We also tested the advection-diffusion-reaction model with the assumption that the N_2O reduction rate is proportional to the concentration of both N_2O and electron donors (see section I of auxiliary material Text S1). Although the second model contains large uncertainties in POC concentration, the estimated isotopomeric enrichment factors agree with those of the model based on N_2O concentration within errors.

[25] We estimated isotopomeric enrichment factors for N_2O reduction (see Table 2 and Figure 5 for the results) by applying a vertical advection-diffusion-reaction model to the N_2O concentration and isotopomer ratios over the depth range 400–700 m at the ETNP site. Current physical oceanographic theory suggests that the predominant form of ventilation in the oceans below the mixed layer is mixing along isopycnal surfaces [*Ledwell et al.*, 1993; *Luyten et al.*, 1983]. Enrichment factors for nitrate reduction by denitrification estimated by lateral reaction-diffusion models ($\varepsilon = -30 \pm 3‰$ [*Brandes et al.*, 1998]; $\varepsilon = -30 \pm 7.5‰$ [*Voss et al.*, 2001]) are identical within the range of the errors to those estimated using vertical advection-diffusion-reaction models ($\varepsilon = -30 \pm 5‰$: [*Sutka et al.*, 2004b] [see also *Cline and Kaplan*, 1975]). The agreement between these results on nitrate suggests that our estimate of the enrichment factors for N_2O should be reliable in the ETNP.

[26] The enrichment factor was estimated at $-11.6 \pm 1.0‰$ for the bulk (average) N, $-19.8 \pm 2.3‰$ for the center N (α-site nitrogen), $-3.4 \pm 0.3‰$ for the end N (β-site nitrogen), $-30.5 \pm 3.2‰$ for the ^{18}O of N_2O (Table 2). The range of the enrichment factors is based on a sensitivity test (see Appendix A). Our estimated enrichment factors of bulk nitrogen and oxygen for N_2O reduction are within the range of reported values (Table 2). Our enrichment factor of bulk nitrogen is similar to that of *Barford et al.* [1999] ($-12.9‰$), which was estimated using pure cultures of a denitrifier, *Paracoccus denitrificans*, grown under steady state in a chemostat. *Ostrom et al.* [2007] also estimated the enrichment factor of bulk nitrogen, using a denitrifier, *Paracoccus denitrificans,* as $-10.9‰$. The oxygen isotopic enrichment factor of our estimation is similar to that of *Wahlen and Yoshinari* [1985] ($-37‰$), which was estimated by pure cultures of a denitrifier, *Paracoccus aeruginosa,* grown in batch culture. The ratio of oxygen to nitrogen isotope fractionation at 400–700 m at the ETNP site ($\varepsilon_{18O}/\varepsilon_{bulk\text{-}N} = 2.58 \pm 0.08$; see Table 2 for details) is similar to the ratios of N_2O reduction by a denitrifier, *Paracoccus denitrificans* ($\varepsilon_{18O}/\varepsilon_{bulk\text{-}N} = 2.28$ [*Ostrom et al.*, 2007]), and soils ($\varepsilon_{18O}/\varepsilon_{bulk\text{-}N} = 2.5$ [*Ostrom et al.*, 2007], 2.51–2.56 [*Menyailo and Hungate*, 2006], and 2.0 [*Mandernack et al.*, 2000]), although soil incubation experiments give smaller enrichment factors for bulk nitrogen and oxygen. Moreover, the ratio of oxygen to nitrogen enrichment factors ($\varepsilon_{18O}/\varepsilon_{bulk\text{-}N}$) at the ETNP site is also similar to the isotope fractionation observed in the ETNP ($\Delta\delta^{18}O/\Delta\delta^{15}N^{bulk} \approx 2$) and in the Arabian Sea ($\Delta\delta^{18}O/\Delta\delta^{15}N^{bulk} \approx 3$) [*Yoshinari et al.*, 1997].

[27] A constant 1:1 ratio of $^{15}N/^{14}N$ and $^{18}O/^{16}O$ isotope fractionation in nitrate has been observed during denitrification [*Durka et al.*, 1994; *Bottcher et al.*, 1990; *Sigman et al.*, 2005] and nitrate assimilation by marine phytoplankton [*Granger et al.*, 2004]. *Granger et al.* [2004] suggested that total isotope fractionation in phytoplankton consists of two steps, namely reversible flow across the membrane of a cell (first step) and enzyme reaction (second step), and that isotope fractionation for diffusion of substrates into and out of a cell is negligible. The two-step model has also been suggested to explain nitrogen isotope fractionation for nitrate reduction by denitrifiers [*Mariotti et al.*, 1982; *Ostrom et al.*, 2002, *Sigman et al.*, 2005, 2006]. This two-step model, which is similar to the two-step models describing carbon isotope fractionation [e.g., *Laws et al.*, 1995], could also apply to isotopomer fractionation for N_2O reduction by denitrifiers as follows:

$$A \underset{F_{ba},\,\varepsilon_{ba}}{\overset{F_{ab},\,\varepsilon_{ab}}{\rightleftharpoons}} B \xrightarrow{F_{bc},\varepsilon_{bc}} C \qquad (20)$$

Assuming steady state, there are steady flows, F_{ab}, F_{ba}, and F_{bc} from A to B, from B to A, and from B to C, respectively. Isotopomeric enrichment factors are described as ε_{ab}, ε_{ba}, and ε_{bc}, respectively, for each step. In case of N_2O reduction, A is N_2O outside a cell, B is N_2O inside a cell, and C is the N_2 inside a cell. Then, isotopomeric enrichment factor for N_2O reduction can be calculated by the equation of *Rees* [1973],

$$\varepsilon_{N2OR} = \varepsilon_{ac} = \varepsilon_{ab} + (\varepsilon_{bc} - \varepsilon_{ba})X_b \qquad (0 \le X_b \le 1), \qquad (21)$$

where $X_b = F_{ba}/F_{ab}$.

Isotope fractionations for diffusion of nitrate [*Bryan et al.*, 1983; *Granger et al.*, 2004; *Mariotti et al.*, 1982], N_2 [*Handley and Raven*, 1992], and CO_2 [*Farquhar et al.*, 1982; *O'Leary*, 1984] through the cell membrane (ε_{ab} and ε_{ba}) are thought to be negligible. Assuming that isotopomer fractionations for diffusion (ε_{ab} and ε_{ba}) of N_2O are also negligible, the ratios between isotopomeric enrichment factors for N_2O reduction are constant, even if the ratio X_b changes. The steady state denitrifier model of *Barford et al.* [1999] (see section 2.4 for details) estimates the isotopic enrichment factors for enzyme reaction (ε_{bc}). Similarity of nitrogen isotopic enrichment factors estimated by *Barford et al.* [1999] (ε_{bc}) and this study (ε_{ac}) suggests that the ratio X_b at 400–700 m at the ETNP site is close to 1 (equation (21) estimates the ratio X_b.).

4.3. Estimating the Contribution of Nitrifiers and Denitrifiers to N_2O Production

[28] We analyzed the contribution of nitrifiers and denitrifiers to N_2O production at the ETNP and GOC sites using SP-$\delta^{15}N^{bulk}$ plot (see section 2.4 for description and see Figure 6

Table 2. Isotopomeric Enrichment Factors for N_2O Reduction[a]

Isotopomeric enrichment factor, ‰						
$\varepsilon_{bulk\text{-}N}$	ε_{α}	ε_{β}	ε_{180}	$\varepsilon_{180}/\varepsilon_{bulk\text{-}N}$[b]	Conditions	Reference
−11.6 ± 1.0	−19.8 ± 2.3	−3.4 ± 0.3	−30.5 ± 3.2	2.58 ± 0.08	eastern tropical North Pacific (advection-diffusion-reaction models)	this study (400–700 m in the ETNP)
−6.9– −9.8			−12.6– −24.9	2.51	incubation of soil collected under larch in Siberia	*Menyailo and Hungate* [2006]
−6.3– −8.3			−16– −21	2.55– 2.56	incubation of soil collected under birch in Siberia	*Menyailo and Hungate* [2006]
−12.9[c]	...	...	...	...	chemostat culture of *Paracoccus denitrificans*	*Barford et al.* [1999]
−39	...	...	...	...	pure culture of *Azotobacter vinelandii* at 25°C[d]	*Yamazaki et al.* [1987]
...	...	...	−42	...	pure culture of *Pseudomonas aeruginosa* at 10°C	*Wahlen and Yoshinari* [1985]
...	...	...	−37	...	pure culture of *Pseudomonas aeruginosa* at 26°C	*Wahlen and Yoshinari* [1985]
−2.4	...	...	−4.9	2.0	incubation of landfill soil in ambient air at 24°C	*Mandernack et al.* [2000]
...	...	...	...	~2	correlation between $\delta^{15}N^{bulk}$ and $\delta^{18}O$ in N_2O dissolved in the eastern tropical North Pacific	*Yoshinari et al.* [1997]
...	...	...	...	~3	correlation between $\delta^{15}N^{bulk}$ and $\delta^{18}O$ in N_2O dissolved in the Arabian Sea	*Yoshinari et al.* [1997]

[a] $N_2O \rightarrow N_2$.
[b] The ratio of $\varepsilon_{18O}/\varepsilon_{bulk\text{-}N}$ is equivalent to the slope of the regression line on $\delta^{18}O$ versus $\delta^{15}N$ plot (n = 4, R^2 = 0.998). The error of $\varepsilon_{18O}/\varepsilon_{bulk\text{-}N}$ is equivalent to the error of the slope of the regression line.
[c] Average value of replicate experiments.
[d] A N_2-fixing bacterium.

for the results). For the SP-$\delta^{15}N^{bulk}$ analysis, we calculated the isotopomer ratios of N_2O released by denitrifiers ($\boldsymbol{\delta}$-$N_2O_{D\text{-}rel}$) and adopted the reference value estimated by *Popp et al.* [2002] for the isotopomer ratios of N_2O released by nitrifiers ($\boldsymbol{\delta}$-$N_2O_{N\text{-}pro}$) (see Tables 3a and 3b for detail calculations). We estimated the range of nitrogen isotope ratio in nitrate in the ETNP and GOC on the basis of previous studies at the depth of our observations (see references in Table 3a). The value of $\boldsymbol{\delta}$-$N_2O_{D\text{-}rel}$ was calculated using equations (16) and (17), and isotopomeric enrichment factors of ε_{NaR} ($NO_3^- \rightarrow N_2O$) and ε_{N2OR} ($N_2O \rightarrow N_2$) listed in Table 3b. Variation of $\boldsymbol{\delta}$-$N_2O_{D\text{-}rel}$ was determined using a propagation of error calculation.

[29] There are two choices for the isotopomer ratios of N_2O produced by nitrifiers ($\boldsymbol{\delta}$-$N_2O_{N\text{-}pro}$): estimation based

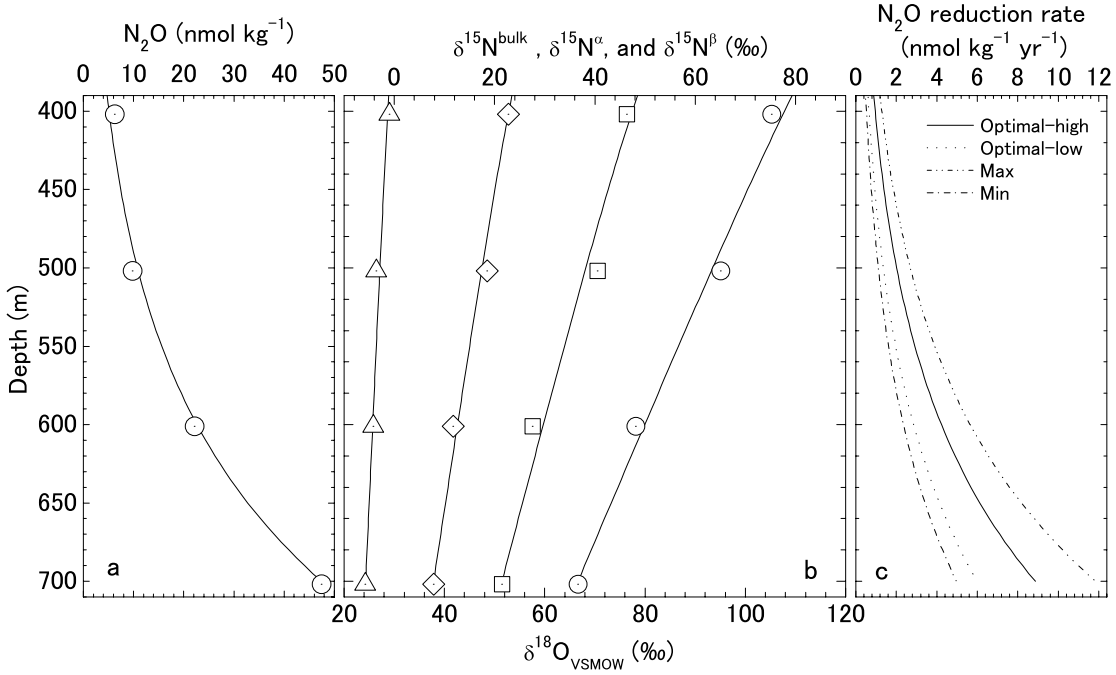

Figure 5. (a) Concentration and (b) isotopomer ratios of N_2O at the ETNP site versus depth. Solid lines are best fit, advection-diffusion-reaction model results. Figure 5a shows observed concentration (open circle), and Figure 5 b shows $\delta^{15}N^{bulk}$ (open diamond), $\delta^{15}N^{\alpha}$ (open square), $\delta^{15}N^{\beta}$ (open triangle), and $\delta^{18}O$ (open circle) of observed N_2O. (c) N_2O reduction rates calculated by the model with different values of diffusion coefficient (K) and advection velocity (V). The values of V/K and V for each curve named in legend are listed in Table A1. The solid curve named as "Optimal-high" is the "best fit" result using the values of V/K = -1.4×10^{-3} m^{-1} and V = −4.0 m yr^{-1}.

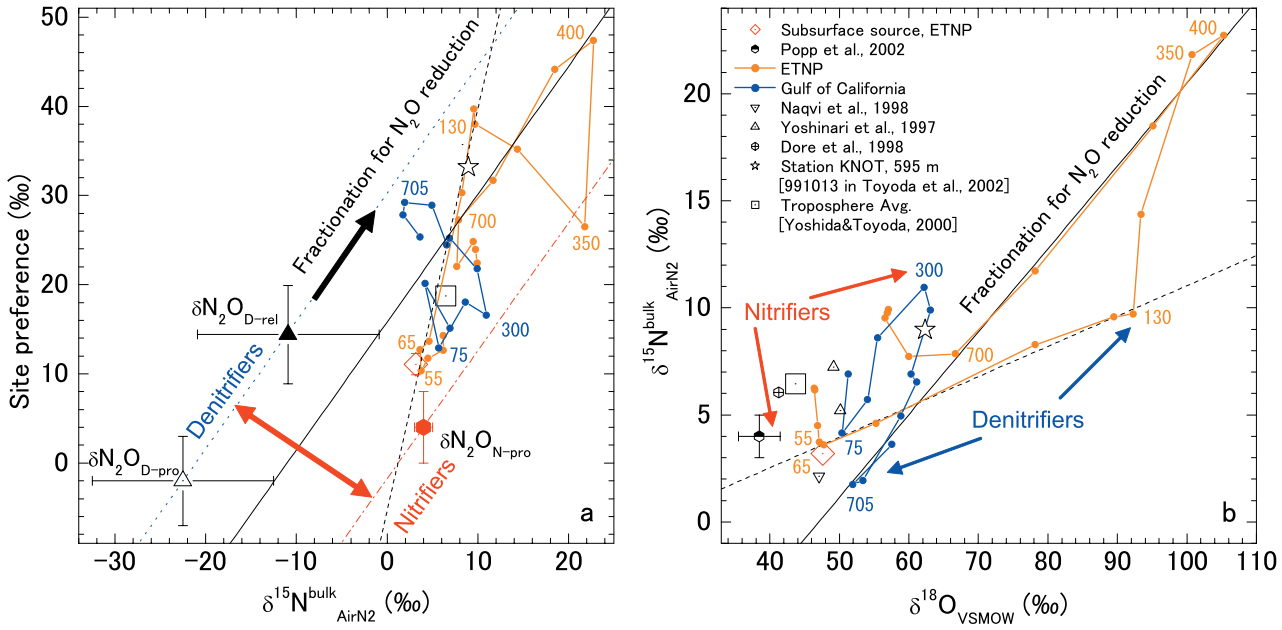

Figure 6. Plots of (a) ^{15}N-site preference versus $\delta^{15}N^{bulk}$ and (b) $\delta^{15}N^{bulk}$ versus $\delta^{18}O$. Symbols representing the observations and previous reports are defined in legend. Figure 6a shows isotopomer ratios of N_2O produced by nitrifiers (red pentagon) and denitrifiers (open triangle), and isotopomer ratios of N_2O released from denitrifiers (solid triangle). Red dash-dotted line and blue dotted line are in parallel with the isotopomer fractionation for N_2O reduction. In Figures 6a and 6b, orange and blue numbers are the depths for each sample at the ETNP and GC sites, respectively. Black solid line and broken line are the regression lines between 400 and 700 m and between 65 and 130 m, respectively, at the ETNP site. All isotopic values are expressed as permil (‰) deviations from atmospheric N_2 (for nitrogen) and VSMOW (for oxygen).

on isotopomer analysis of N_2O produced presumably by nitrifier-denitrification in the shallow aphotic zone in the subtropical North Pacific Gyre [*Popp et al.*, 2002] or calculation using isotopomeric enrichment factors estimated from pure cultures [*Sutka et al.*, 2006, 2003,2004a]. *Sutka et al.* [2006, 2003, 2004a] found that for pure culture experiments SP of N_2O is close to 0‰ when N_2O is produced via nitrite by nitrite reductase and that SP of N_2O is around 30‰ when N_2O is produced by NH_2OH oxidation. At station ALOHA (22°45′N, 158°00′W) in the aphotic zone in the subtropical North Pacific Gyre, SP of N_2O produced in situ was estimated at ~4‰ [*Popp et al.*, 2002]. The low SP observed in this subsurface layer at station ALOHA and the ETNP site is consistent with the production of N_2O by nitrifier denitrification as observed in pure culture experiments by *Sutka et al.* [2006, 2003, 2004a]. Comparison of $\delta^{18}O$-N_2O with $\delta^{18}O$-O_2 also indicates the contribution of nitrifier denitrification for N_2O production at the depth of 350–500 m at station ALOHA [*Ostrom et al.*, 2000; *Popp et al.*, 2002]. However, we do not adopt the SP of 0‰ for nitrifier denitrification as the end-member of $\boldsymbol{\delta}$-$N_2O_{N\text{-}pro}$, because we could not exclude the possibility of contribution of NH_2OH oxidation to N_2O production in the aerobic oceans. It is also difficult to use isotopic enrichment factors for the N_2O production by nitrifiers, because there are no data for nitrogen isotope ratios of substrates available and, furthermore, calculation of the nitrogen isotope ratio of N_2O produced by marine nitrifiers using isotopic enrichment factors is not straightforward. *Casciotti et al.* [2002] found that the extent of isotope fractionation

Table 3a. Estimates of Isotopomer Ratios of N_2O Released From Nitrifiers and Denitrifiers

Isotopomer Ratios, ‰	Symbol	$\delta^{15}N$	SP	Notes
Nitrate in the eastern tropical North Pacific and Gulf of California	$\boldsymbol{\delta}$-NO_3^-	7.5 ± 6.5	0	the eastern tropical North Pacific: *Brandes et al.* [1998], *Cline and Kaplan* [1975], *Sigman et al.* [2005], *Sutka et al.* [2004b], and *Voss et al.* [2001]; the Gulf of California: *Altabet et al.* [1999][a]
N_2O produced by denitrifiers	$\boldsymbol{\delta}$-$N_2O_{D\text{-}pro}$	−22.5 ± 10.0	−2 ± 5[b]	$\boldsymbol{\delta}$-$N_2O_{D\text{-}pro}$ = $\boldsymbol{\delta}$-NO_3^- + ε_{NaR}
N_2O released from denitrifiers	$\boldsymbol{\delta}$-$N_2O_{D\text{-}rel}$	−10.9 ± 10.0	14.4 ± 5.5[b]	$\boldsymbol{\delta}$-N_2O_{D-rel} = $\boldsymbol{\delta}$-$N_{2D\text{-}pro}$ − εN_{2OR}
N_2O produced by nitrifiers	$\boldsymbol{\delta}$-$N_2O_{N\text{-}pro}$	4 ± 1	4 ± 4	N_2O produced in the subsurface layer in the subtropical North Pacific Gyre [*Popp et al.*, 2002]

[a] The data at the depth of 200–600 m is excluded for the eastern tropical North Pacific because nitrate at the depth should not be the substrate of the N_2O that we analyze.

[b] Range of the value is calculated from propagation of errors: $\sigma(A) = [\{\sigma(B)\}^2 + \{\sigma(C)\}^2]^{(1/2)}$ when A = B + C.

Table 3b. Isotopomeric Enrichment Factors for the Calculation of N_2O Isotopomer Ratios of Sources

Isotopomeric Enrichment Factors, ‰	Symbol	$\varepsilon_{bulk\text{-}N}$	ε_{SP}[a]	Notes
Nitrate reduction by denitrifiers: $NO_3^- \rightarrow N_2O$	δ_{NaR}	-30 ± 7.5	-2 ± 5	$\varepsilon_{bulk\text{-}N}$: lateral diffusion-reaction model in the ETNP [*Brandes et al.*, 1998; *Voss et al.*, 2001] and vertical advection-diffusion-reaction model in the ETNP [*Cline and Kaplan*, 1975; *Sutka et al.*, 2004b], ε_{SP}: pure culture of denitrifiers: *Pseudomonas chlororaphis, Pseudomonas aurelofaciens* [*Sutka et al.*, 2006], and *Paracoccus denitrificans* [*Toyoda et al.*, 2005]
N_2O reduction by denitrifiers: $N_2O \rightarrow N_2$	δ_{N2OR}	-11.6 ± 1.0	-16.4 ± 2.3	Vertical advection-diffusion-reaction model in the ETNP (this study)

[a] ε_{SP} is calculated by the following equation: $\varepsilon_{sp} = 2\ \varepsilon_{\alpha} - 2\ \varepsilon_{bulk\text{-}N}$. Range of the value is calculated from propagation of errors: $\sigma(SP) = \{4\ \sigma(\delta^{15}N^{\alpha})^2 + 4\ \sigma(\delta^{15}N^{bulk})^2\}^{1/2}$.

for ammonia oxidation by marine nitrifiers is about 10–25‰ smaller than that of a terrestrial nitrifier such as *Nitrosospira tenuis* and a well-studied nitrifier, *Nitrosomonas europaea*. Therefore, considering the difficulties in estimating the value for $\boldsymbol{\delta}$-$N_2O_{N\text{-}pro}$ using isotopomer enrichment factors and the consistency in isotopic values observed in ocean environments, we adopt the isotopomer ratios of N_2O produced in situ in the aerobic subsurface layer in the subtropical North Pacific Gyre [*Popp et al.*, 2002] as the value of δ-$N_2O_{N\text{-}pro}$ (Table 3a).

[30] To calculate the isotopomer ratios of N_2O released from denitrifiers ($\boldsymbol{\delta}$-$N_2O_{D\text{-}rel}$), we assumed that the ratio X_b in the two-step model is one. Then we applied our estimated enrichment factor ε_{N2OR}(= ε_{ac}; $N_2O_{situ} \rightarrow N_2$) to ε_{bc} ($N_2O_{vivo} \rightarrow N_2$) of the steady state denitrifier model to calculate $\boldsymbol{\delta}$-$N_2O_{D\text{-}rel}$ (Table 3b). However, even if the ratio X_b is far from one, the slope of SP to $\delta^{15}N^{bulk}$ is constant. Thus the ratio X_b should not affect the analysis of the origin of N_2O.

[31] The isotopomer ratios of N_2O at 700 m at the GOC site and at 120 m at the ETNP site plot close to the isotopomer fractionation line for N_2O reduction from δ-$N_2O_{D\text{-}rel}$ (blue dotted line at Figure 6a), which suggests that N_2O is released from and consumed by denitrifiers in these water masses. On the contrary, the isotopomer ratios of N_2O dissolved at the N_2O concentration maximum (~65 m) at the ETNP site and the suboxic zone above the OMZ (~300 m) at the GOC site plot close to the isotopomer fractionation line of N_2O reduction from δ-$N_2O_{N\text{-}pro}$ (red dash-dotted line at Figure 6a), which suggests that N_2O is mainly released from nitrifiers in these water masses.

[32] We estimated the contribution ratio of N_2O production by nitrifiers to the total N_2O emission (N-ratio) and its error using equation 19 and propagation of error, respectively. Quantitative analysis indicates that 71 ± 17% of the dissolved N_2O is released from nitrifiers at the subsurface N_2O maximum (at 65 m) at the ETNP site. In the suboxic zone under the core of the OMZ (at 800 m) at the ETNP site, the estimated N-ratio was 60 ± 21%. Nitrifiers primarily contribute to N_2O production at 55 m at the ETNP site (N-ratio = 79 ± 15%), and at 75 m at the GOC site (N-ratio = 80 ± 15%). The model results are consistent with the minimum SP values found at these depths, which is a signal of nitrifier-denitrification (Figures 2b and 2e), and with the nitrite concentration peak, a signal of ammonia oxidation by ammonia oxidizers (Figure 2c). N-ratios were also estimated at 92 ± 13% and 11 ± 43% at 300 m and 700 m at the GOC site, respectively.

[33] In order to resolve the contribution of each process more precisely, evaluation of the tropospheric N_2O is necessary in subsurface layers and aerobic waters. In contrast, in suboxic zones where N_2O is produced and consumed by denitrification, the modern and preindustrial tropospheric N_2O should be consumed and thus should not influence the estimates of the N-ratio. Although there are large variations in δ^{15}N-nitrate and isotopic/isotopomeric enrichment factors (see references listed in notes in Tables 3a and 3b), we applied unique values for the end-members, $\boldsymbol{\delta}$-$N_2O_{N\text{-}pro}$ and $\boldsymbol{\delta}$-$N_2O_{D\text{-}rel}$, for estimating N-ratios using SP-$\delta^{15}N^{bulk}$ analysis. The large errors in N-ratios can be attributed to the wide range of the end-member values of $\boldsymbol{\delta}$-$N_2O_{D\text{-}rel}$. To reduce errors in $\boldsymbol{\delta}$-$N_2O_{D\text{-}rel}$, it is essential to constrain the error in δ^{15}N-nitrate and the nitrogen isotopic enrichment factor for nitrate reduction. Furthermore, even though we estimated errors in N-ratios, there remains additional uncertainty relating to the end-member of $\boldsymbol{\delta}$-$N_2O_{N\text{-}pro}$. It is essential to establish a methodology for estimating the end-member of $\boldsymbol{\delta}$-$N_2O_{N\text{-}pro}$ in the oceans. Given the influence of diffusion and advection on the distribution of N_2O and nitrate, it is insufficient to use δ^{15}N-nitrate at each point as the substrate of N_2O. In future studies, it is desirable to estimate the N-ratio using an advection-diffusion-reaction model with distribution of isotope ratios of substrates and isotopic/isotopomeric enrichment factors, which are functions of the concentrations of substrates and environmental parameters related to microbial activities such as temperature.

[34] We also plotted the isotopomer ratios of N_2O at the concentration maximum (600 m) at Station KNOT in the western North Pacific (data for 991013 from *Toyoda et al.* [2002]) as the open black star on Figure 6a. Considering that δ^{15}N-NO_3^- in the northern part of the North Pacific is ~5‰ [*Casciotti et al.*, 2002] and that the value of δ^{15}N-NO_3^- is within the range of δ^{15}N-NO_3^- for the SP-$\delta^{15}N^{bulk}$ analysis (7.5 ± 6.5‰), the contribution of each process to N_2O production at Station KNOT can be resolved using a plot of SP versus $\delta^{15}N^{bulk}$ (Figure 6a). The SP-$\delta^{15}N^{bulk}$ plot indicates that denitrification dominates N_2O production in the OMZ at Station KNOT in the North Pacific (N-ratio = 31 ± 34%). Thus isotopomer analysis of N_2O with steady state model for denitrifiers supports the denitrification hypothesis of *Yamagishi et al.* [2005] and *Yoshida et al.* [1989]. Isotopomer analysis of N_2O has a potential to resolve the dispute between the nitrification and denitrification hypotheses for the N_2O cycle in the oceans.

[35] The production and consumption processes of N_2O indicated by the SP-$\delta^{15}N^{bulk}$ analysis are consistent with the processes indicated by N* values and the concentrations of nitrite and oxygen. However, the conventional analysis of $\delta^{15}N^{bulk}$ and $\delta^{18}O$ of N_2O at the GOC site leads to the opposite conclusion: the smaller $\delta^{15}N^{bulk}$ and $\delta^{18}O$ at 700 m than those at 300 m indicates that contribution of nitrification at 700 m is larger than that at 300 m (Figure 6b). This suggestion is not consistent with N* and O_2 concentration (Figures 2d and 2f). Therefore the analysis of bulk nitrogen and oxygen isotope ratios may not be an effective tool for resolving production processes of N_2O under suboxic conditions in the oceans. In contrast, the plot of the SP versus $\delta^{15}N^{bulk}$ is very useful for resolving production and consumption processes.

5. Conclusions and Implications

[36] In the ETNP, N_2O is mainly produced by nitrifiers at the concentration maximum (60–80 m deep) located at the subsurface oxycline. Isotopomer ratios of N_2O produced at the maximum are 3.2 ± 0.1, 8.7 ± 0.6, −2.3 ± 0.6, 47.6 ± 0.3, and 11.0 ± 1.2‰ (1σ, n = 5) for $\delta^{15}N^{bulk}$, $\delta^{15}N^{\alpha}$, $\delta^{15}N^{\beta}$, $\delta^{18}O$, and ^{15}N-site preference, respectively. At the bottom of the subsurface N_2O concentration peak, N_2O is produced and consumed by denitrifiers. At the suboxic zone under the OMZ at 800 m, N_2O is strongly consumed by denitrifiers after release by nitrifiers and denitrifiers. In the Gulf of California, N_2O is dominantly produced by nitrifiers from the subsurface to 300 m. At the N_2O concentration maximum at the lower OMZ (700 m), N_2O is produced and consumed by denitrifiers.

[37] Isotopomeric fractionation for N_2O reduction was analyzed using a one-dimensional, vertical advection-diffusion-reaction model over the depth range 400–700 m in the ETNP OMZ, where N_2O diffuses and advects from the suboxic zone under the OMZ at 800 m and where N_2O is only consumed by denitrifiers. Isotopomeric enrichment factors for N_2O reduction were estimated to be −11.6 ± 1.0, −19.8±2.3, −3.4 ± 0.3, and −30.5 ± 3.2‰ for $\delta^{15}N^{bulk}$, $\delta^{15}N^{\alpha}$, $\delta^{15}N^{\beta}$, and $\delta^{18}O$, respectively. Isotopomer analysis of N_2O with isotopomeric enrichment factors is a powerful tool for estimating the ratios of N_2O released from nitrifiers and denitrifiers in the oceans. Isotopomer analysis of N_2O suggests that conventional bulk nitrogen and oxygen isotope ratios cannot effectively differentiate the N_2O released from denitrifiers and marine nitrifiers in the low-oxygen regions although the analysis on the plot of $\delta^{15}N$ versus $\delta^{18}O$ gives information on the extent of its consumption. Thus isotopomer analysis is a powerful tool for resolving the N_2O cycle in the oceans.

[38] Isotopomer ratios of N_2O will be a sensitive signal of N_2O reduction, namely N_2 production, by denitrification, which is the main process of N loss from the oceans. Our plot of ^{15}N-site preference versus $\delta^{15}N^{bulk}$ indicates that water masses under suboxic conditions in the ETNP, Gulf of California, and even in the OMZ in the western North Pacific show evidence of N loss by denitrification. The suggestion of N loss from the northern Pacific Ocean is consistent with the suggestion by *Li and Peng* [2002], who estimated remineralization ratios in the northern Pacific from nutrient and oxygen concentrations using a three-part mixing model. They argued that the low N/P ratio for the northern Pacific basins indicates that organic nitrogen is converted partly into gaseous N_2O and N_2 through nitrification or denitrification processes in low-oxygen regions, or in the reducing microenvironments of organic matter within an oxygenated water column. N* has been used as a signal of N loss in the oceans. However, N* is affected by several factors such as nitrogen fixation, remineralization ratio of nutrients, and the amount of DON that has not been remineralized. Isotopomer analysis of N_2O will be a useful tool for resolving the distributions of water masses that have lost nitrogen by denitrification.

Table A1. Parameters for the Advection-Diffusion-Reaction Model

Name	10^3 V/K, m^{-1}	V, m yr^{-1}
Optimal-high	−1.4	−4.0
Optimal-low	−1.4	−2.7
Maximum	−1.0	−4.0
Minimum	−1.8	−2.7

Appendix A: Model Parameters and Sensitivity Test

A1. Ratio of Advection Velocity to Eddy Diffusion Coefficient (V/K)

[39] We estimated the value of V/K using the one dimensional, advection-diffusion model of *Tsunogai* [1972] and *Munk* [1966] with the potential temperature from our cruise (170–810 m at the ETNP site). We selected this depth range because of a highly linear mixing line exists on a T-S diagram. The value of V/K was $-1.4 \pm 0.4 \times 10^{-3}$ m^{-1}.

A2. Advection Velocity (V)

[40] We adopt the advection velocity estimated by *Chung and Craig* [1973] using ^{226}Ra. The velocities in the z direction are −2.7 m yr^{-1} for minimum and −4.0 m yr^{-1} for maximum at Station SCAN X-56 (08°07′N, 113°55′W; Bottom = 4035 m), which is close to our ETNP site (16°10′N, 106°59′W).

A3. N_2O Reduction Rate (F_z)

[41] The reaction rate constant of m was estimated by fitting the concentration model (equations (1) and (2)) to the measured N_2O concentration between 400 and 700 m (O_2 < 1 μmol kg^{-1}) at the ETNP site, as shown in Figure 5a. The value of m was estimated to make an asymptotic curve close to 0 nmol kg^{-1} at 0 m. Several results of the N_2O reduction rate are shown in Figure 5c.

A4. Sensitivity

[42] Sensitivity was tested to estimate the range of enrichment factors. The fractionation factor was dependent mainly on the shape of the curve fit to the N_2O concentration profile. The values of the parameters (V/K and V) were varied within their ranges to estimate errors of the fractionation factors. We used parameters of ''Optimal-high,'' as shown in Table A1, for estimating the optimal factors. Shifting the value of V did not change the estimated value of fractionation factors. The range of N_2O reduction

rates was also estimated. Estimated profiles were shown in Figure 5c, and sets of parameters are shown in Table A1.

[43] **Acknowledgments.** We thank Nils Napp for dissolved O_2 measurements, and all scientists working on the EPREX for help with sample collection in the ETNP. We are indebted to A. W. Graham for dissolved O_2 measurement, sample collection, and cruise information including CTD data from the Gulf of California. We wish to thank the crew of the R/V *Revelle* for assistance on our cruise in the ETNP, and to thank the crew of the R/V *New Horizon* for assistance on the cruise in the Gulf of California. We are indebted to H. Nara for advice on the advection-diffusion-reaction model and for his comments on this paper, and to T. Rust and F. J. Sansone for assistance in this research. We thank R. L. Sutka and N. E. Ostrom for interlaboratory calibration of N_2O isotopomer ratios. We also thank R. L. Sutka, J. van-Haren, L. Farıacute;as, N. Handa, J. P. Montoya, and Y. H. Li for valuable discussions. This research was supported by U.S. National Science Foundation grants OCE 9817064 (BNP, Francis J. Sansone and Edward A. Laws) and OCE 0240787 (BNP). Reviews by N. E. Ostrom and two anonymous reviewers were very helpful in improving this paper. This is SOEST contribution 7021.

References

Altabet, M. A., C. Pilskaln, R. Thunell, C. Pride, D. Sigman, F. Chavez, and R. Francois (1999), The nitrogen isotope biogeochemistry of sinking particles from the margin of the eastern North Pacific, *Deep Sea Res., Part I*, *46*, 655–679.

Barford, C. C., J. P. Montoya, M. A. Altabet, and R. Mitchell (1999), Steady-state nitrogen isotope effects of N_2 and N_2O production in *Paracoccus denitrificans*, *Appl. Environ. Microbiol.*, *65*, 989–994.

Bottcher, J., O. Strebel, S. Voerkelius, and H. L. Schmidt (1990), Using isotope fractionation of nitrate nitrogen and nitrate oxygen for evaluation of microbial denitrification in a sandy aquifer, *J. Hydrol.*, *114*(3–4), 413–424.

Boyer, T. P., C. Stephens, J. I. Antonov, M. E. Conkright, R. A. Locarnini, T. D. O'Brien, and H. E. Garcia (2002), *World Ocean Atlas 2001*, vol. 2, *Salinity* [CD-ROM], edited by S. Levitus, *NOAA Atlas NESDIS 50*, Natl. Oceanic and Atmos. Admin., Silver Spring, Md.

Brandes, J. A., A. H. Devol, T. Yoshinari, D. A. Jayakumar, and S. W. A. Naqvi (1998), Isotopic composition of nitrate in the central Arabian Sea and eastern tropical North Pacific: A tracer for mixing and nitrogen cycles, *Limnol. Oceanogr.*, *43*(7), 1680–1689.

Brenninkmeijer, C. A. M., and T. Rockmann (1999), Mass spectrometry of the intramolecular nitrogen isotope distribution of environmental nitrous oxide using fragment-ion analysis, *Rapid Commun. Mass Spectrom.*, *13*(20), 2028–2033.

Bryan, B. A., G. Shearer, J. L. Skeeters, and D. H. Kohl (1983), Variable expression of the nitrogen isotope effect associated with denitrification of nitrite, *J. Biol. Chem.*, *258*(14), 8613–8617.

Casciotti, K. L., D. M. Sigman, M. G. Hastings, J. K. Bohlke, and A. Hilkert (2002), Measurement of the oxygen isotopic composition of nitrate in seawater and freshwater using the denitrifier method, *Anal. Chem.*, *74*(19), 4905–4912.

Casciotti, K. L., D. M. Sigman, and B. B. Ward (2003), Linking diversity and stable isotope fractionation in ammonia-oxidizing bacteria, *Geomicrobiol. J.*, *20*(4), 335–353.

Castro, C. G., F. P. Chavez, and C. A. Collins (2001), Role of the California Undercurrent in the export of denitrified waters from the eastern tropical North Pacific, *Global Biogeochem. Cycles*, *15*(4), 819–830.

Chung, Y.-C., and H. Craig (1973), Radium-226 in the eastern equatorial Pacific, *Earth Planet. Sci. Lett.*, *17*, 306–318.

Cline, J. D., and I. R. Kaplan (1975), Isotopic fractionation of dissolved nitrate during denitrification in the eastern tropical North Pacific Ocean, *Mar. Chem.*, *3*, 271–299.

Codispoti, L. A., J. W. Elkins, T. Yoshinari, G. Fredrich, C. Sakamoto, and T. Packard (1992), On the nitrous oxide flux from productive regions that contain low oxygen waters, in *Oceanography of the Indian Ocean*, edited by B. Desai, pp. 271–284, Oxford Univ. Press, New York.

Cohen, Y., and L. I. Gordon (1978), Nitrous oxide production in the oxygen minimum of the eastern tropical North Pacific: Evidence for its consumption during denitrification and possible mechanisms for its production, *Deep Sea Res.*, *25*, 509–524.

Conkright, M. E., H. E. Garcia, T. D. O'Brien, R. A. Locarnini, T. P. Boyer, C. Stephens, and J. I. Antonov (2002), *World Ocean Atlas 2001,* vol. 4, *Nutrients* [CD-ROM], edited by S. Levitus, *NOAA Atlas NESDIS 52*, Natl. Oceanic and Atmos. Admin., Silver Spring, Md.

Crutzen, P. J. (1970), The influence of nitrogen oxides on the atmospheric ozone content, *Q. J. R. Meteorol. Soc.*, *96*, 320–325.

Deutsch, C., A. Ganachaud, N. Gruber, R. M. Key, and J. L. Sarmiento (2001), Denitrification and N_2 fixation in the Pacific Ocean, *Global Biogeochem. Cycles*, *15*(2), 483–506.

Dore, J. E., B. N. Popp, D. M. Karl, and F. J. Sansone (1998), A large source of atmospheric nitrous oxide from subtropical North Pacific surface waters, *Nature*, *396*, 63–66.

Durka, W., E. D. Schulze, G. Gebauer, and S. Voerkelius (1994), Effects of forest decline on uptake and leaching of deposited nitrate determined from N^{15} and O^{18} measurements, *Nature*, *372*, 765–767.

Farquhar, G. D., and J. A. Berry (1982), On the relationship between carbon isotope discrimination and the inter-cellular carbon-dioxide concentration in leaves, *Aust. J. Plant Physiol.*, *9*, 121–137.

Granger, J., D. M. Sigman, J. A. Needoba, and P. J. Harrison (2004), Coupled nitrogen and oxygen isotope fractionation of nitrate during assimilation by cultures of marine phytoplankton, *Limnol. Oceanogr.*, *49*(5), 1763–1773.

Grasshoff, K., M. Ehrhardt, and K. Kremling (Eds.) (1983), *Methods of Seawater Analysis,* 2nd rev. and extended ed., pp. 61–72, 143–150, Verlag Chemie, New York.

Gruber, N., and J. L. Sarmiento (1997), Global patterns of marine nitrogen fixation and denitrification, *Global Biogeochem. Cycles*, *11*(2), 235–266.

Handley, L. L., and J. A. Raven (1992), The use of natural abundance of nitrogen isotopes in plant physiology, *Plant Cell Environ.*, *15*, 965–985.

Intergovernmental Panel on Climate Change (2001), Atmospheric chemistry and greenhouse gases, in *Climate Change 2001: The Scientific Basis*, edited by J. T. Houghton et al., pp. 241–287, Cambridge Univ. Press, New York.

Jones, R. D. (1991), An improved fluorescence method for the determination of nanomolar concentrations of ammonium in natural waters, *Limnol. Oceanogr.*, *36*(4), 814–819.

Jørgensen, K. S., H. B. Jensen, and J. Sørensen (1984), Nitrous oxide reduction from nitrification and denitrification in marine sediment at low oxygen concentrations, *Can. J. Microbiol.*, *30*, 1073–1078.

Kaiser, J., T. Röckmann, and C. A. M. Brenninkmeijer (2003), Complete and accurate mass spectrometric isotope analysis of tropospheric nitrous oxide, *J. Geophys. Res.*, *108*(D15), 4476, doi:10.1029/2003JD003613.

Laws, E. A., B. N. Popp, R. R. Bidigare, M. C. Kennicutt, and S. A. Macko (1995), Dependence of phytoplankton carbon isotopic composition on growth-rate and $[CO_2]_{aq}$: Theoretical considerations and experimental results, *Geochim. Cosmochim. Acta*, *59*, 1131–1138.

Ledwell, J. R., A. J. Watson, and C. S. Law (1993), Evidence for slow mixing across the pycnocline from an open-ocean tracer-release experiment, *Nature*, *364*, 701–703.

Li, Y. H., and T. H. Peng (2002), Latitudinal change of remineralization ratios in the oceans and its implication for nutrient cycles, *Global Biogeochem. Cycles*, *16*(4), 1130, doi:10.1029/2001GB001828.

Luyten, J. R., J. Pedlosky, and H. Stommel (1983), The ventilated thermocline, *J. Phys. Oceanogr.*, *13*, 292–309.

Mandernack, K. W., T. Rahn, C. Kinney, and M. Wahlen (2000), The biogeochemical controls of the $\delta^{15}N$ and $\delta^{18}O$ of N_2O produced in landfill cover soils, *J. Geophys. Res.*, *105*(D14), 17,709–17,720.

Mariotti, A., J. C. Germon, P. Hubert, P. Kaiser, R. Letolle, A. Tardieux, and P. Tardieux (1981), Experimental determination of nitrogen kinetic isotope fractionation: Some principles; illustration for the denitrification and nitrification processes, *Plant Soil*, *62*, 413–430.

Mariotti, A., J. C. Germon, A. Leclerc, G. Catroux, and R. Letolle (1982), Experimental determination of kinetic isotope fractionation of nitrogen isotopes during denitrification, in *Stable Isotopes*, edited by H.-L. Schmidt et al., pp. 459–464, Elsevier, New York.

Menyailo, O. V., and B. A. Hungate (2006), Stable isotope discrimination during soil denitrification: Production and consumption of nitrous oxide, *Global Biogeochem. Cycles*, *20*, GB3025, doi:10.1029/2005GB002527.

Munk, W. H. (1966), Abyssal recipes, *Deep Sea Res*, *13*, 707–730.

Naqvi, S. W. A., T. Yoshinari, D. A. Jayakumar, M. A. Altabet, P. V. Narvekar, A. H. Devol, J. A. Brandes, and L. A. Codispoti (1998), Budgetary and biogeochemical implications of N_2O isotope signatures in the Arabian Sea, *Nature*, *394*, 462–464.

Nevison, C. D., R. F. Weiss, and I. D. J. Erickson (1995), Global oceanic emissions of nitrous oxide, *J. Geophys. Res.*, *100*(C8), 15,809–15,820.

Nevison, C., J. H. Butler, and J. W. Elkins (2003), Global distribution of N_2O and the ΔN_2O-AOU yield in the subsurface ocean, *Global Biogeochem. Cycles*, *17*(4), 1119, doi:10.1029/2003GB002068.

O'Leary, M. H. (1984), Measurement of the isotope fractionation associated with diffusion of carbon-dioxide in aqueous-solution, *J. Phys. Chem.*, *88*, 823–825.

Ostrom, N. E., M. E. Russ, B. Popp, T. M. Rust, and D. M. Karl (2000), Mechanisms of nitrous oxide production in the subtropical North Pacific based on determinations of the isotopic abundances of nitrous oxide and di-oxygen, *Chemosphere Global Change Sci.*, *2*(3–4), 281–290.

Ostrom, N. E., L. O. Hedin, J. C. von Fischer, and G. P. Robertson (2002), Nitrogen transformations and NO_3^- removal at a soil-stream interface: A stable isotope approach, *Ecol. Appl.*, *12*(4), 1027–1043.

Ostrom, N. E., A. Pitt, R. Sutka, P. H. Ostrom, A. S. Grandy, K. M. Huizinga, and G. P. Robertson (2007), Isotopologue effects during N_2O reduction in soils and in pure cultures of denitrifiers, *J. Geophys. Res.*, doi:10.1029/2006JG000287, in press.

Pataki, D. E., J. R. Ehleringer, L. B. Flanagan, D. Yakir, D. R. Bowling, C. J. Still, N. Buchmann, J. O. Kaplan, and J. A. Berry (2003), The application and interpretation of Keeling plots in terrestrial carbon cycle research, *Global Biogeochem. Cycles*, *17*(1), 1022, doi:10.1029/2001GB001850.

Pierotti, D., and R. A. Rasmussen (1980), Nitrous oxide measurements in the eastern tropical Pacific Ocean, *Tellus*, *32*(1), 56–72.

Popp, B. N., et al. (2002), Nitrogen and oxygen isotopomeric constraints on the origins and sea-to-air flux of N_2O in the oligotrophic subtropical North Pacific gyre, *Global Biogeochem. Cycles*, *16*(4), 1064, doi:10.1029/2001GB001806.

Poth, M., and D. D. Focht (1985), ^{15}N kinetic analysis of N_2O production by Nitrosomonas europaea: An examination of nitrifier denitrification, *Appl. Environ. Microbiol.*, *49*, 1134–1141.

Prosperie, L. F., L. A. Codispoti, S. W. A. Naqvi, J. Aftab, D. Mastern, R. Patrick, and R. Williams (1996), Oxygen deficient (suboxic) conditions in the Arabian Sea, *Eos Trans. AGU*, *77*(3), Ocean Sci. Meet. Suppl., OS11A-15.

Ramanathan, V., R. J. Cicerone, H. B. Singh, and J. T. Kiehl (1985), Trace gas trends and their potential role in climate change, *J. Geophys. Res.*, *90*(D3), 5547–5566.

Rees, C. E. (1973), A steady-state model for sulphur isotope fractionation in bacterial reduction processes, *Geochim. Cosmochim. Acta*, *37*, 1141–1162.

Ritchie, G. A. F., and D. J. D. Nicholas (1972), Identification of nitrous oxide produced by oxidative and reductive processes in Nitrosomonas europaea, *Biochem. J.*, *126*, 1181–1191.

Sansone, F. J., B. N. Popp, A. Gasc, A. W. Graham, and T. M. Rust (2001), Highly elevated methane in the eastern tropical North Pacific and associated isotopically enriched fluxes to the atmosphere, *Geophys. Res. Lett.*, *28*(24), 4567–4570.

Shearer, G., and D. H. Kohl (1988), Nitrogen isotopic fractionation and ^{18}O exchange in relation to the mechanism of denitrification of nitrite by Pseudomonas stutzeri, *J. Biol. Chem.*, *263*(26), 13,231–13,245.

Sigman, D. M., J. Granger, P. J. DiFiore, M. M. Lehmann, R. Ho, G. Cane, and A. van Geen (2005), Coupled nitrogen and oxygen isotope measurements of nitrate along the eastern North Pacific margin, *Global Biogeochem. Cycles*, *19*, GB4022, doi:10.1029/2005GB002458.

Sigman, D. M., J. Granger, P. J. DiFiore, M. F. Lehmann, R. Ho, G. Cane, and A. van Geen (2006), Correction to "Coupled nitrogen and oxygen isotope measurements of nitrate along the eastern North Pacific margin", *Global Biogeochem. Cycles*, *20*, GB1005, doi:10.1029/2005GB002682.

Stephens, C., J. I. Antonov, T. P. Boyer, M. E. Conkright, R. A. Locarnini, T. D. O'Brien, and H. E. Garcia (2002), *World Ocean Atlas 2001,* vol. 1, *Temperature* [CD-ROM], edited by S. Levitus, *NOAA Atlas NESDIS 49*, Natl. Oceanic and Atmos. Admin., Silver Spring, Md.

Suntharalingam, P., and J. L. Sarmiento (2000), Factors governing the oceanic nitrous oxide distribution: Simulations with an ocean general circulation model, *Global Biogeochem. Cycles*, *14*(1), 429–454.

Suntharalingam, P., J. L. Sarmiento, and J. R. Toggweiler (2000), Global significance of nitrous-oxide production and transport from oceanic low-oxygen zones: A modeling study, *Global Biogeochem. Cycles*, *14*(4), 1353–1370.

Suthhof, A., V. Ittekkot, and B. Gaye-Haake (2001), Millennial-scale oscillation of denitrification intensity in the Arabian Sea during the late Quaternary and its potential influence on atmospheric N_2O and global climate, *Global Biogeochem. Cycles*, *15*(3), 637–649.

Sutka, R. L., N. E. Ostrom, P. H. Ostrom, H. Gandhi, and J. A. Breznak (2003), Nitrogen isotopomer site preference of N_2O produced by *Nitrosomonas europaea* and *Methylococcus capsulatus* Bath, *Rapid Commun. Mass Spectrom.*, *17*(7), 738–745.

Sutka, R. L., N. E. Ostrom, P. H. Ostrom, H. Gandhi, and J. A. Breznak (2004a), Erratum, Nitrogen isotopomer site preference of N_2O produced by *Nitrosomonas europaea* and *Methylococcus capsulatus* Bath, *Rapid Commun. Mass Spectrom.*, *18*(12), 1411–1412.

Sutka, R. L., N. E. Ostrom, P. H. Ostrom, and M. S. Phanikumar (2004b), Stable nitrogen isotope dynamics of dissolved nitrate in a transect from the North Pacific Subtropical Gyre to the Eastern Tropical North Pacific, *Geochim. Cosmochim. Acta*, *68*, 517–527.

Sutka, R. L., N. E. Ostrom, P. H. Ostrom, J. A. Breznak, H. Gandhi, A. J. Pitt, and F. Li (2006), Distinguishing nitrous oxide production from nitrification and denitrification on the basis of isotopomer abundances, *Appl. Environ. Microbiol.*, *72*, 638–644.

Toyoda, S., and N. Yoshida (1999), Determination of nitrogen isotopomers of nitrous oxide on a modified isotope ratio mass spectrometer, *Anal. Chem.*, *71*(20), 4711–4718.

Toyoda, S., N. Yoshida, T. Miwa, Y. Matsui, H. Yamagishi, U. Tsunogai, Y. Nojiri, and N. Tsurushima (2002), Production mechanism and global budget of N_2O inferred from its isotopomers in the western North Pacific, *Geophys. Res. Lett.*, *29*(3), 1037, doi:10.1029/2001GL014311.

Toyoda, S., H. Mutobe, H. Yamagishi, N. Yoshida, and Y. Tanji (2005), Fractionation of N_2O isotopomers during production by denitrifier, *Soil Biol. Biochem.*, *37*(8), 1535–1545, doi:10.1016/j.soilbio.2005.01.009.

Tsunogai, S. (1972), An estimate of the vertical diffusivity of the deep water., *J. Oceanogr. Soc. Jpn.*, *28*, 145–152.

Voss, M., J. W. Dippner, and J. P. Montoya (2001), Nitrogen isotope patterns in the oxygen-deficient waters of the Eastern Tropical North Pacific Ocean, *Deep Sea Res.*, *Part I*, *48*, 1905–1921.

Wahlen, M., and T. Yoshinari (1985), Oxygen isotope ratios in N_2O from different environments, *Nature*, *313*, 780–782.

Weiss, R. F., and B. A. Price (1980), Nitrous oxide solubility in water and seawater, *Mar. Chem.*, *8*, 347–359.

Westley, M. B., B. N. Popp, T. M. Rust, and F. J. Sansone (2001), Sources and isotopic compositions of nitrous oxide in the subtropical North Pacific and the eastern tropical North Pacific, in *Proceedings of the First International Symposium on Isotopomers*, edited by N. Yoshida, pp. 169–175, Jpn. Sci. and Technol. Agency, Yokohama, Japan.

Westley, M. B., H. Yamagishi, B. N. Popp, and N. Yoshida (2006), Nitrous oxide cycling in the Black Sea inferred from stable isotope and isotopomer distributions, *Deep Sea Res., Part*, *53*, 1802, doi:10.1016/j.dsr2.2006.03.012.

Wrage, N., G. L. Velthof, M. L. van Beusichem, and O. Oenema (2001), Role of nitrifier denitrification in the production of nitrous oxide, *Soil Biol. Biochem.*, *33*(12–13), 1723–1732.

Wyrtki, K. (1962), The oxygen minima in relation to ocean circulation, *Deep Sea Res.*, *9*, 11–23.

Yamagishi, H., N. Yoshida, S. Toyoda, B. N. Popp, M. B. Westley, and S. Watanabe (2005), Contributions of denitrification and mixing on the distribution of nitrous oxide in the North Pacific, *Geophys. Res. Lett.*, *32*, L04603, doi:10.1029/2004GL021458.

Yamazaki, T., N. Yoshida, E. Wada, and S. Matsuo (1987), N_2O reduction by Azotobacter vinelandii with emphasis on kinetic nitrogen isotope effects, *Plant Cell Physiol.*, *28*, 263–271.

Yoshida, N., and S. Toyoda (2000), Constraining the atmospheric N_2O budget from intramolecular site preference in N_2O isotopomers, *Nature*, *405*, 330–334.

Yoshida, N., E. Wada, A. Hattori, T. Saino, and S. Matsuo (1984), $^{15}N/^{14}N$ ratio of dissolved N_2O in the eastern tropical Pacific Ocean, *Nature*, *307*, 442–444.

Yoshida, N., H. Morimoto, M. Hirano, I. Koike, S. Matsuo, E. Wada, T. Saino, and A. Hattori (1989), Nitrification rates and ^{15}N abundances of N_2O and NO_3^- in the western North Pacific, *Nature*, *342*, 895–897.

Yoshinari, T., M. A. Altabet, S. W. A. Naqvi, L. Codispoti, A. Jayakumar, M. Kuhland, and A. Devol (1997), Nitrogen and oxygen isotopic composition of N_2O from suboxic waters of the eastern tropical North Pacific and the Arabian Sea – measurement by continuous-flow isotope-ratio monitoring, *Mar. Chem.*, *56*, 253–264.

K. Koba, Institute of Symbiotic Science and Technology, Tokyo University of Agriculture and Technology, Saiwai-cho 3-5-8, Fuchu-city, Tokyo 1838-509, Japan. (keikoba@cc.tuat.ac.jp)

B. N. Popp, Department of Geology and Geophysics, School of Ocean and Earth Science and Technology, University of Hawaii, 1680 East-West Road, Honolulu, HI 96822, USA. (popp@hawaii.edu)

S. Toyoda, Department of Environmental Chemistry and Engineering, Interdisciplinary Graduate School of Science and Engineering, Tokyo Institute of Technology, Mail-Box G1-17, 4259 Nagatsuta, Midori-ku, Yokohama 226-8502, Japan. (toyoda.s.aa@m.titech.ac.jp)

S. Watanabe, Mutsu Institute for Oceanography, Japan Agency for Marine-Earth Science and Technology, 690 Kitasekine, Sekine, Mutsu 035-0022, Japan. (swata@jamstec.go.jp)

M. B. Westley, Geophysical Fluid Dynamics Laboratory, National Oceanic and Atmospheric Administration, 201 Forrestal Road, Princeton, NJ 08540-6649, USA. (marian.westley@noaa.gov)

H. Yamagishi, Atmospheric Environmental Division, National Institute for Environmental Studies, 16-2 Onogawa, Tsukuba, Ibaraki 305-8506, Japan. (yamagishi.hiroaki@nies.go.jp)

Y. Yamanaka, Faculty of Environmental Earth Science, Hokkaido University, N10W5, Sapporo, Hokkaido 060-0810, Japan. (galapen@ees.hokudai.ac.jp)

N. Yoshida, Frontier Collaborative Research Center, Tokyo Institute of Technology, G1-25, 4259 Nagatsuta, Midori-ku, Yokohama 226-8502, Japan. (naoyoshi@depe.titech.ac.jp)